Journal of Computational Physics 253 (2013) 189–208

Contents lists available at SciVerse ScienceDirect

Journal of Computational Physics

www.elsevier.com/locate/jcp

Efficient numerical methods for computing ground states of spin-1 Bose–Einstein condensates based on their characterizations

Weizhu Bao [a], I-Liang Chern [b,c], Yanzhi Zhang [d,*]

[a] Department of Mathematics and Center for Computational Science and Engineering, National University of Singapore, Singapore 119076, Singapore
[b] Department of Applied Mathematics and Center of Mathematical Modeling and Scientific Computing, National Chiao Tung University, Hsinchu 30010, Taiwan
[c] Department of Mathematics, National Taiwan University, Taipei 10617, Taiwan
[d] Department of Mathematics and Statistics, Missouri University of Science and Technology, Rolla, MO 65409-0020, USA

ARTICLE INFO

Article history:
Received 18 May 2012
Received in revised form 24 April 2013
Accepted 27 June 2013
Available online 10 July 2013

Keywords:
Spin-1 Bose–Einstein condensate
Ground state
Ferromagnetic
Antiferromagnetic
Single-mode approximation
Gradient flow with discrete normalization

ABSTRACT

In this paper, we propose efficient numerical methods for computing ground states of spin-1 Bose–Einstein condensates (BECs) with/without the Ioffe–Pritchard magnetic field $B(\mathbf{x})$. When $B(\mathbf{x}) \neq 0$, a numerical method is introduced to compute the ground states and it is also applied to study properties of ground states. Numerical results suggest that the densities of $m_F = \pm 1$ components in ground states are identical for any nonzero $B(\mathbf{x})$. In particular, if $B(\mathbf{x}) \equiv B \neq 0$ is a constant, the ground states satisfy the single-mode approximation. When $B(\mathbf{x}) \equiv 0$, efficient and simpler numerical methods are presented to solve the ground states of spin-1 BECs based on their ferromagnetic/antiferromagnetic characterizations. Numerical simulations show that our methods are more efficient than those in the literature. In addition, some conjectures are made from our numerical observations.

1. Introduction

Since its first realization in 1995, Bose–Einstein condensation (BEC) has become an important tool to investigate behaviors of quantum many-body system. In earlier BEC experiments, atoms were confined in a magnetic trap, where their spin degree of freedom was frozen [1,12]. Recently, the development of optical trapping techniques has enabled to confine atoms independently of their spin orientation and thus result in so-called spinor condensates. The spinor BEC has revealed numerous exciting new phenomena which are not possessed by single-component (spin-frozen) condensates. It has provided a unique possibility of exploring fundamental concepts of quantum mechanics in a remarkably controllable and tunable environment [32,33,31].

In the mean-field approximation, a spin-F ($F \in \mathbb{N}$) condensate can be described by coupled Gross–Pitaevskii equations (CGPEs) consisting of $2F+1$ equations, and each of them governs one of the $2F+1$ Zeeman states ($m_F = -F, -F+1, \ldots, F-1, F$). For example, a spin-1 BEC is described by the following dimensionless CGPEs [14,27,8,6,7,32]:

* Corresponding author.
E-mail addresses: mathbaowz@nus.edu.sg (W. Bao), chern@math.nctu.edu.tw (I-L. Chern), zhangyanz@mst.edu (Y. Zhang).
URL: http://www.math.nus.edu.sg/~bao/ (W. Bao).

0021-9991/$ – see front matter
http://dx.doi.org/10.1016/j.jcp.2013.06.036

$$
\begin{aligned}
i\frac{\partial\psi_1(\mathbf{x},t)}{\partial t} &= \big[H+\beta_s\big(|\psi_1|^2+|\psi_0|^2-|\psi_{-1}|^2\big)\big]\psi_1+\beta_s\psi_0^2\psi_{-1}^*+B\psi_0,\\
i\frac{\partial\psi_0(\mathbf{x},t)}{\partial t} &= \big[H+\beta_s\big(|\psi_1|^2+|\psi_{-1}|^2\big)\big]\psi_0+2\beta_s\psi_1\psi_0^*\psi_{-1}+B^*\psi_1+B\psi_{-1},\\
i\frac{\partial\psi_{-1}(\mathbf{x},t)}{\partial t} &= \big[H+\beta_s\big(|\psi_{-1}|^2+|\psi_0|^2-|\psi_1|^2\big)\big]\psi_{-1}+\beta_s\psi_0^2\psi_1^*+B^*\psi_0,
\end{aligned}
\tag{1.1}
$$

where $\mathbf{x}\in\mathbb{R}^d$ (for $d=1,2$ or 3) is the Cartesian coordinate vector, $t\geqslant 0$ is time and $\psi_j(\mathbf{x},t)$ is the complex-valued wave function of the j-th ($j=1,0,-1$) component. The operator H is defined by

$$
H=-\frac{1}{2}\nabla^2+V_d(\mathbf{x})+\beta_n\sum_{j=-1}^{1}|\psi_j|^2,
\tag{1.2}
$$

where $V_d(\mathbf{x})$ represents a d-dimensional external trapping potential and it is determined by the type of system under investigation. For instance, if a three-dimensional (3D) harmonic potential is considered, it takes the form $V_3(\mathbf{x})=\frac{1}{2}(\gamma_x^2x^2+\gamma_y^2y^2+\gamma_z^2z^2)$ with γ_x, γ_y and γ_z being the dimensionless trapping frequencies in x-, y- and z-directions, respectively. The constants β_n and β_s describe the spin-independent interaction and spin-exchange interaction, respectively, and they are proportional to the total number of atoms N. If $\beta_n>0$ (resp. <0), the spin-independent interaction is repulsive (resp. attractive), while when $\beta_s>0$ (resp. <0), the spin-exchange interaction is antiferromagnetic (resp. ferromagnetic). The dimensionless function $B(\mathbf{x})\in\mathbb{C}$ represents the external Ioffe–Pritchard magnetic field [13,16,18]. In addition, f^* represents the complex conjugate of a function f.

There are two important invariants of (1.1): the *normalization of the wave functions*, i.e.,

$$
\big\|\Psi(\cdot,t)\big\|^2=\sum_{j=-1}^{1}\big\|\psi_j(\cdot,t)\big\|^2:=\sum_{j=-1}^{1}\int_{\mathbb{R}^d}\big|\psi_j(\mathbf{x},t)\big|^2\,d\mathbf{x}\equiv\big\|\Psi(\cdot,0)\big\|^2=1,\quad t\geqslant 0,
\tag{1.3}
$$

with $\Psi(\mathbf{x},t)=(\psi_1(\mathbf{x},t),\psi_0(\mathbf{x},t),\psi_{-1}(\mathbf{x},t))^T$, and the *energy*

$$
E\big(\Psi(\cdot,t)\big):=E_0\big(\Psi(\cdot,t)\big)+2\,\mathrm{Re}\bigg(\int_{\mathbb{R}^d}B\big(\psi_1^*\psi_0+\psi_0^*\psi_{-1}\big)\,d\mathbf{x}\bigg)\equiv E\big(\Psi(\cdot,0)\big),\quad t\geqslant 0,
\tag{1.4}
$$

with $\mathrm{Re}(f)$ denoting the real part of a function f and

$$
\begin{aligned}
E_0\big(\Psi(\cdot,t)\big):=\int_{\mathbb{R}^d}\bigg[&\sum_{j=-1}^{1}\bigg(\frac{1}{2}|\nabla\psi_j|^2+V_d(\mathbf{x})|\psi_j|^2\bigg)+\frac{\beta_n}{2}\big(|\psi_1|^2+|\psi_0|^2+|\psi_{-1}|^2\big)^2\\
&+\frac{\beta_s}{2}\big(|\psi_1|^2-|\psi_{-1}|^2\big)^2+\beta_s|\psi_0|^2\big(|\psi_1|^2+|\psi_{-1}|^2\big)+2\beta_s\,\mathrm{Re}\big(\psi_1^*\psi_0^2\psi_{-1}^*\big)\bigg]d\mathbf{x},
\end{aligned}
\tag{1.5}
$$

for $t\geqslant 0$, i.e., $E_0(\Psi(\cdot,t))$ represents the energy when $B(\mathbf{x})\equiv 0$. In the case of $B(\mathbf{x})\equiv 0$, the energy $E_0(\Psi(\cdot,t))$ is also conserved, i.e.,

$$
E_0\big(\Psi(\cdot,t)\big)\equiv E_0\big(\Psi(\cdot,0)\big),\quad t\geqslant 0,\ \text{when } B(\mathbf{x})\equiv 0.
\tag{1.6}
$$

Furthermore, the *total magnetization* is conserved when $B(\mathbf{x})\equiv 0$, i.e.,

$$
M\big(\Psi(\cdot,t)\big):=\int_{\mathbb{R}^d}\big(\big|\psi_1(\mathbf{x},t)\big|^2-\big|\psi_{-1}(\mathbf{x},t)\big|^2\big)\,d\mathbf{x}\equiv M\big(\Psi(\cdot,0)\big)=M,\quad t\geqslant 0,
\tag{1.7}
$$

with $-1\leqslant M\leqslant 1$.

Ground state, a stationary state with the lowest energy, plays an important role in understanding the properties of BECs. There have been many experimental and mathematical studies on ground states of spin-1 condensates. In [30], the phase diagram of the ground states of spin-1 BECs was first reported in the Thomas–Fermi regimes. The phenomena of broken axisymmetry phase were observed in [26] for spin-1 ferromagnetic condensates. Recently, Matuszewski et al. compared the phase separation of the ground states in the ferromagnetic and antiferromagnetic systems [22,23]. Cao et al. proved the existence of the ground states in one-dimensional condensates [9]. On the other hand, some numerical methods have been proposed in recent literature to compute ground states of spin-1 BECs in the absence of the external Ioffe–Pritchard magnetic field (i.e., $B(\mathbf{x})\equiv 0$ in (1.1)). For instance, Bao and Wang proposed in [6] a continuous normalized gradient flow (CNGF) and constructed a Crank–Nicolson finite difference scheme to discretize it. In [7,19], Bao and Lim introduced a gradient flow with discrete normalization (GFDN) and they used the sine pseudo-spectral method to discretize it. It has

been pointed out in [7] that GFDN type method is computationally more efficient than CNGF in [6]. Chen et al. proposed a pseudo-arclength continuation method to compute the ground states of spin-1 BECs [10]. To the best of our knowledge, all these methods focus on computing the ground states of spin-1 BECs where $B(\mathbf{x}) = 0$ and so far there are still no numerical reports about the ground states when $B(\mathbf{x}) \neq 0$. In addition, to obtain the ground states in the cases of $B(\mathbf{x}) = 0$, all the available methods solve three-component CGPE type equations, which makes the simulations very costly. We notice that when $B(\mathbf{x}) = 0$, the ground states of spin-1 BECs can be simplified to a single-mode (resp. two-component) reduction for ferromagnetic (resp. antiferromagnetic) systems [17,34,20]. Thus, the ground states in this case can be effectively found by solving the reduced single or two-component systems instead of the original three-component one.

In this paper, we propose (i) a numerical method for computing ground states of spin-1 BECs when $B(\mathbf{x}) \neq 0$; (ii) efficient and simpler methods for the case when $B(\mathbf{x}) \equiv 0$, by taking into account their ferromagnetic and antiferromagnetic characterizations. It is organized as follows. In Section 2, we propose a numerical method to compute the ground states when the Ioffe–Pritchard magnetic field $B(\mathbf{x}) \neq 0$. While when $B(\mathbf{x}) \equiv 0$, the ground states of the three-component system (1.1) are characterized by those of the corresponding reduced systems, i.e., the single-mode and two-component reductions for the ferromagnetic and antiferromagnetic condensates, respectively. The reductions of the ground states for ferromagnetic and antiferromagnetic spin-1 BECs are discussed in Section 3, followed by their numerical discretizations. Numerical results of ground states as well as comparison between different methods are presented in Section 4. In Section 5, we draw some conclusions and conjectures based on our numerical observations.

2. Numerical methods for ground states with nonzero B

Some numerical methods have been recently proposed in the literature [6,7,19,10] to compute ground states of spin-1 BECs in the absence of the Ioffe–Pritchard magnetic field $B(\mathbf{x})$. However, there is still no numerical report on the ground states when $B(\mathbf{x}) \neq 0$. In this section, we propose a numerical method for computing ground states of spin-1 BECs with nonzero $B(\mathbf{x})$.

When $B(\mathbf{x}) \neq 0$, the ground state $\Phi_g(\mathbf{x}) = (\phi_{1,g}(\mathbf{x}), \phi_{0,g}(\mathbf{x}), \phi_{-1,g}(\mathbf{x}))^T$ is defined by minimizing the energy functional E in (1.4) subject to the normalization of wave functions in (1.3), i.e.,

Find $(\Phi_g \in S)$, such that

$$E_g := E(\Phi_g) = \min_{\Phi \in S} E(\Phi), \tag{2.1}$$

where the set S is defined by

$$S := \left\{ \Phi = (\phi_1, \phi_0, \phi_{-1})^T \;\middle|\; \|\Phi\|^2 = 1,\ E(\Phi) < \infty \right\}.$$

It is easy to see that the ground state Φ_g defined in (2.1) satisfies the following Euler–Lagrange equations

$$\begin{aligned}
&\mu\phi_1(\mathbf{x}) = \left[H + \beta_s\left(|\phi_1|^2 + |\phi_0|^2 - |\phi_{-1}|^2\right)\right]\phi_1 + \beta_s\phi_0^2\phi_{-1}^* + B\phi_0,\\
&\mu\phi_0(\mathbf{x}) = \left[H + \beta_s\left(|\phi_1|^2 + |\phi_{-1}|^2\right)\right]\phi_0 + 2\beta_s\phi_1\phi_0^*\phi_{-1} + B^*\phi_1 + B\phi_{-1}, \quad \mathbf{x} \in \mathbb{R}^d,\\
&\mu\phi_{-1}(\mathbf{x}) = \left[H + \beta_s\left(|\phi_{-1}|^2 + |\phi_0|^2 - |\phi_1|^2\right)\right]\phi_{-1} + \beta_s\phi_0^2\phi_1^* + B^*\phi_0,
\end{aligned} \tag{2.2}$$

with the constraint of normalization

$$\left\|\Phi(\cdot)\right\|^2 = \int_{\mathbb{R}^d} \left(\left|\phi_1(\mathbf{x})\right|^2 + \left|\phi_0(\mathbf{x})\right|^2 + \left|\phi_{-1}(\mathbf{x})\right|^2\right) d\mathbf{x} = 1, \tag{2.3}$$

where the operator H is defined in (1.2). The eigenvalue μ is the Lagrange multiplier (or called *chemical potential*) corresponding to the constraint in (2.3), which can be computed from its eigenfunction Φ by

$$\begin{aligned}
\mu := \mu(\Phi) = E(\Phi) + \int_{\mathbb{R}^d} \Bigg[&\frac{\beta_n}{2}\left(|\phi_1|^2 + |\phi_0|^2 + |\phi_{-1}|^2\right)^2 + \frac{\beta_s}{2}\left(|\phi_1|^2 - |\phi_{-1}|^2\right)^2\\
&+ \beta_s|\phi_0|^2\left(|\phi_1|^2 + |\phi_{-1}|^2\right) + 2\beta_s\,\mathrm{Re}\left(\phi_1^*\phi_0^2\phi_{-1}^*\right)\Bigg] d\mathbf{x}.
\end{aligned}$$

In fact, the Euler–Lagrange equations in (2.2) can also be obtained from the time-dependent GPEs in (1.1) by substituting the ansatz

$$\psi_j(\mathbf{x}, t) = e^{-i\mu t}\phi_j(\mathbf{x}), \quad j = 1, 0, -1. \tag{2.4}$$

The eigenfunctions Φ of the constrained nonlinear eigenvalue problem (2.2)–(2.3) are usually called *stationary states* of spin-1 BECs. Among all stationary states, the eigenfunctions with minimum energy is called the *ground state* and those with larger energies are usually called *excited states*.

Various algorithms have been proposed in the literature to find minimizers of the energy functional under constraints. While the imaginary time method (i.e., replacing t with $-i\tau$ in (1.1)) is one of the most popular approaches in studying the ground states of BECs. It can be mathematically justified by the normalized gradient flow [11,3]. In this paper, we will develop our numerical methods for computing ground states of spin-1 BECs based on the gradient flow with discrete normalization; see more information in [3]. Choose a time step $\Delta t > 0$ and define the time sequence as $t_n = n\Delta t$ for $n = 0, 1, \ldots$. Then in each time interval $[t_n, t_{n+1}]$, the gradient flow with discrete normalization (GFDN) is given by

$$\begin{aligned}
\frac{\partial \phi_1(\mathbf{x},t)}{\partial t} &= -\big[H + \beta_s\big(|\phi_1|^2 + |\phi_0|^2 - |\phi_{-1}|^2\big)\big]\phi_1 - \beta_s\phi_0^2\phi_{-1}^* - B\phi_0,\\
\frac{\partial \phi_0(\mathbf{x},t)}{\partial t} &= -\big[H + \beta_s\big(|\phi_1|^2 + |\phi_{-1}|^2\big)\big]\phi_0 - 2\beta_s\phi_1\phi_0^*\phi_{-1} - B^*\phi_1 - B\phi_{-1},\\
\frac{\partial \phi_{-1}(\mathbf{x},t)}{\partial t} &= -\big[H + \beta_s\big(|\phi_{-1}|^2 + |\phi_0|^2 - |\phi_1|^2\big)\big]\phi_{-1} - \beta_s\phi_0^2\phi_1^* - B^*\phi_0,
\end{aligned} \tag{2.5}$$

followed by a projection step as

$$\phi_j\big(\mathbf{x}, t_{n+1}^+\big) := \frac{\phi_j(\mathbf{x}, t_{n+1}^-)}{\|\Phi(\cdot, t_{n+1}^-)\|}, \quad j = 1, 0, -1, \tag{2.6}$$

where $\phi_j(\mathbf{x}, t_{n+1}^\pm) = \lim_{t\to t_{n+1}^\pm} \phi_j(\mathbf{x}, t)$ $(j = 1, 0, -1)$. The gradient flow in (2.5)–(2.6) can be viewed as first applying the steepest descent method to the energy functional in (1.4) without constraint and then projecting the solution back to the unit sphere to satisfy the normalization constraint in (2.3).

In order to solve the GFDN numerically, we discretize (2.5) by using the sine pseudo-spectral method for spatial derivatives and the backward/forward Euler scheme for linear/nonlinear terms of temporal derivatives [4,35]. In the following, we will give a detailed description of our numerical method. Notice that because of the confinement of the external trapping potentials, the wave function Φ in (2.5) decays to zero exponentially fast when $|\mathbf{x}| \to \infty$. Thus, in practical computations we can truncate the problem into a bounded computational domain Ω with homogeneous Dirichlet boundary conditions, i.e.,

$$\phi_j(\mathbf{x}, t)|_{\partial\Omega} = 0, \quad t \geqslant 0, \ j = 1, 0, -1. \tag{2.7}$$

For simplicity of notations, we will only present the scheme in one-dimensional (1D) cases with a bounded computational domain $\Omega = [a, b]$. Generalizations to higher dimensions are straightforward for tensor product grids. For an even integer $K > 0$, define the spatial mesh size $\Delta x = (b-a)/K > 0$ and grid points $x_k = a + k\Delta x$ for $0 \leqslant k \leqslant K$. Let $\phi_{j,k}^n$ be the numerical approximation of $\phi_j(x_k, t_n)$ and Φ_j^n be a vector consisting of $\phi_{j,k}^n$ for the j-th component. Denote Φ^n a vector with sub-vectors Φ_j^n for $j = 1, 0, -1$. Then over each time interval $[t_n, t_{n+1}]$, we discretize (2.5) as

$$\frac{\phi_{j,k}^{(1)} - \phi_{j,k}^n}{\Delta t} = \frac{1}{2} D_{xx}^s \Phi_j^{(1)}\big|_{x=x_k} - \alpha_j^n\big(\phi_{j,k}^{(1)} - \phi_{j,k}^n\big) + P_{j,k}^n, \quad 1 \leqslant k \leqslant K-1, \tag{2.8}$$

for $j = 1, 0, -1$, where $P_{j,k}^n$ $(j = 1, 0, -1)$ are defined by

$$\begin{aligned}
P_{1,k}^n &:= -\left[V_1(x_k) + \beta_n \sum_{j=-1}^{1} \big|\phi_{j,k}^n\big|^2 + \beta_s\big(\big|\phi_{1,k}^n\big|^2 + \big|\phi_{0,k}^n\big|^2 - \big|\phi_{-1,k}^n\big|^2\big)\right]\phi_{1,k}^n - \beta_s\big(\phi_{0,k}^n\big)^2\big(\phi_{-1,k}^n\big)^* - B(x_k)\phi_{0,k}^n,\\
P_{0,k}^n &:= -\left[V_1(x_k) + \beta_n \sum_{j=-1}^{1} \big|\phi_{j,k}^n\big|^2 + \beta_s\big(\big|\phi_{1,k}^n\big|^2 + \big|\phi_{-1,k}^n\big|^2\big)\right]\phi_{0,k}^n - 2\beta_s\phi_{1,k}^n\big(\phi_{0,k}^n\big)^*\phi_{-1,k}^n - B^*(x_k)\phi_{1,k}^n - B(x_k)\phi_{-1,k}^n,\\
P_{-1,k}^n &:= -\left[V_1(x_k) + \beta_n \sum_{j=-1}^{1} \big|\phi_{j,k}^n\big|^2 + \beta_s\big(\big|\phi_{-1,k}^n\big|^2 + \big|\phi_{0,k}^n\big|^2 - \big|\phi_{1,k}^n\big|^2\big)\right]\phi_{-1,k}^n - \beta_s\big(\phi_{0,k}^n\big)^2\big(\phi_{1,k}^n\big)^* - B^*(x_k)\phi_{0,k}^n.
\end{aligned}$$

D_{xx}^s is a sine pseudo-spectral differential operator approximating ∂_{xx}, which is defined by

$$D_{xx}^s U\big|_{x=x_k} = \sum_{l=1}^{K-1}\big(-\mu_l^2\widehat{U}_l\big)\sin\big(\mu_l(x_k - a)\big), \quad 1 \leqslant k \leqslant K-1, \tag{2.9}$$

where $\widehat{U}_l$ denotes the l-th coefficient of the discrete sine transform of the vector $U = (U_1, U_2, \ldots, U_{K-1})^T$, i.e.,

$$\widehat{U}_l = \frac{2}{K}\sum_{k=1}^{K-1} U_k \sin\big(\mu_l(x_k - a)\big) \quad \text{and} \quad \mu_l = \frac{l\pi}{b-a}, \quad 1 \leqslant l \leqslant K-1.$$

The constant $\alpha_j^n \geqslant 0$ ($j = 1, 0, -1$) is a stabilization parameter, which is chosen in the "optimal" form (such as the time step can be chosen as large as possible) (see, e.g., [35,7,19]).

The projection step in (2.6) is discretized as

$$\phi_{j,k}^{n+1} = \frac{\phi_{j,k}^{(1)}}{\|\Phi^{(1)}\|} \quad \text{with } \|\Phi^{(1)}\| = \sqrt{\Delta x \sum_{j=-1}^{1} \sum_{k=1}^{K-1} |\phi_{j,k}^{(1)}|^2}, \tag{2.10}$$

for $-1 \leqslant j \leqslant 1$ and $1 \leqslant k \leqslant K-1$. In addition, the initial condition is discretized as

$$\phi_{j,k}^0 = \phi_j(x_k, 0), \quad 0 \leqslant k \leqslant K, \ j = 1, 0, -1, \tag{2.11}$$

and the boundary conditions are

$$\phi_{j,0}^n = \phi_{j,K}^n = 0, \quad n = 0, 1, \ldots, \ j = 1, 0, -1. \tag{2.12}$$

The discrete system (2.8), (2.11) and (2.12) can be efficiently solved by the discrete sine transform. In fact, taking the discrete sine transform at both sides of (2.8), we obtain

$$\frac{\widehat{\phi}_{j,l}^{(1)} - \widehat{\phi}_{j,l}^n}{\Delta t} = -\frac{1}{2}\mu_l^2 \widehat{\phi}_{j,l}^{(1)} - \alpha_j^n \big(\widehat{\phi}_{j,l}^{(1)} - \widehat{\phi}_{j,l}^n\big) + \widehat{P}_{j,l}^n, \quad l = 1, 2, \ldots, K-1, \ j = 1, 0, -1, \tag{2.13}$$

which immediately gives that

$$\widehat{\phi}_{j,l}^{(1)} = \frac{(1 + \alpha_j^n \Delta t)\widehat{\phi}_{j,l}^n + \Delta t \widehat{P}_{j,l}^n}{1 + (\alpha_j^n + \mu_l^2/2)\Delta t}, \quad j = 1, 0, -1 \tag{2.14}$$

for $l = 1, 2, \ldots, K-1$ and $n = 0, 1, \ldots$. Since the discrete sine transform is used, the memory required to solve the above system is $O(K)$ and computational cost per time step is $O(K \ln(K))$. The simulation is stopped by requiring that

$$\max_{-1 \leqslant j \leqslant 1} \max_{1 \leqslant k \leqslant K-1} \frac{|\phi_{j,k}^{n+1} - \phi_{j,k}^n|}{\Delta t} < \varepsilon, \tag{2.15}$$

where ε is a chosen small tolerance. The resulting solution $\Phi := \lim_{n\to\infty} \Phi^{n+1}$ is the ground state of the spin-1 BECs.

3. Numerical methods for ground states with $B = 0$

In Section 2, we present a numerical method to compute ground states of spin-1 BECs when $B(\mathbf{x}) \neq 0$, while in this section we will study the ground states when $B(\mathbf{x}) \equiv 0$. In the former case, ground states are minimizers of the energy E in (1.4) under the constraints of normalization in (1.3). However, when $B(\mathbf{x}) \equiv 0$, they also need to satisfy the conservation of magnetization defined in (1.7). In detail, the ground state $\Phi_{0,g}(\mathbf{x})$ when $B(\mathbf{x}) \equiv 0$ is defined by

Find ($\Phi_{0,g} \in S_0$) such that

$$E_{0,g} := E_0(\Phi_{0,g}) = \min_{\Phi \in S_0} E_0(\Phi), \tag{3.1}$$

where E_0 is the energy functional defined in (1.5) and S_0 is a nonconvex set defined as

$$S_0 := \big\{\Phi = (\phi_1, \phi_0, \phi_{-1})^T \ \big| \ \|\Phi(\cdot)\|^2 = 1, \|\phi_1(\cdot)\|^2 - \|\phi_{-1}(\cdot)\|^2 = M, E_0(\Phi) < \infty\big\},$$

with $-1 \leqslant M \leqslant 1$ a given fixed total magnetization. Note that when $\beta_n > 0$, $|\beta_s| \leqslant \beta_n$ and $\lim_{|\mathbf{x}|\to\infty} V_d(\mathbf{x}) = \infty$, the existence of a minimizer of the nonconvex minimization problem (3.1) follows from the standard theory [9,21]. In fact, $E_0(\alpha \cdot \Phi_{0,g}) = E_0(\Phi_{0,g})$ for all constant vector $\alpha = (e^{i\theta_1}, e^{i\theta_0}, e^{i\theta_{-1}})^T$ with $\theta_1 + \theta_{-1} - 2\theta_0 = \pm m\pi$ for any integer m.

Similarly, the ground state $\Phi_{0,g}(\mathbf{x})$ defined in (3.1) also satisfies the following Euler–Lagrange equations:

$$\begin{aligned}
&(\mu + \lambda)\phi_1(\mathbf{x}) = \big[H + \beta_s\big(|\phi_1|^2 + |\phi_0|^2 - |\phi_{-1}|^2\big)\big]\phi_1 + \beta_s \phi_0^2 \phi_{-1}^*,\\
&\mu\phi_0(\mathbf{x}) = \big[H + \beta_s\big(|\phi_1|^2 + |\phi_{-1}|^2\big)\big]\phi_0 + 2\beta_s \phi_1 \phi_0^* \phi_{-1}, \quad \mathbf{x} \in \mathbb{R}^d,\\
&(\mu - \lambda)\phi_{-1}(\mathbf{x}) = \big[H + \beta_s\big(|\phi_{-1}|^2 + |\phi_0|^2 - |\phi_1|^2\big)\big]\phi_{-1} + \beta_s \phi_0^2 \phi_1^*,
\end{aligned} \tag{3.2}$$

with the constraints

$$\|\Phi(\cdot)\|^2 := \sum_{j=-1}^{1} \int_{\mathbb{R}^d} |\phi_j(\mathbf{x})|^2 \, d\mathbf{x} = 1, \qquad \int_{\mathbb{R}^d} \big(|\phi_1(\mathbf{x})|^2 - |\phi_{-1}(\mathbf{x})|^2\big) \, d\mathbf{x} = M, \tag{3.3}$$

where μ and λ are the Lagrange multipliers (or chemical potentials) of the time-independent CGPEs (3.2)–(3.3). The CGPEs in (3.2) can be also obtained from its time-dependent counterpart (1.1) with $B(\mathbf{x}) \equiv 0$ by substituting the ansatz

$$\psi_{\pm1}(\mathbf{x}, t) = e^{-i(\mu\pm\lambda)t}\phi_{\pm1}(\mathbf{x}), \qquad \psi_0(\mathbf{x}, t) = e^{-i\mu t}\phi_0(\mathbf{x}). \tag{3.4}$$

Recently, there have been some numerical methods proposed in the literature (see, e.g., [6,7,19,10]) to compute ground states of spin-1 BECs when $B(\mathbf{x}) = 0$ and all of them directly solve the system of three-component equations. However, we notice that when $B(\mathbf{x}) = 0$, the ground states of spin-1 BECs in fact can be described by a single-mode or two-component reduction based on their ferromagnetic or antiferromagnetic characterizations [20]. As a result, we can introduce numerical methods based on the characterization of spin-1 BECs so as to reduce the computational costs in computing ground states of spin-1 BECs. In the following, we will discuss the ferromagnetic and antiferromagnetic system separately. For each system, we will start with reviewing its characterization properties and then propose numerical methods to solve the reduced system.

3.1. Ferromagnetic system

Experimental observations [17,28,15] and numerical simulations [34,6,7,19] suggest that in ferromagnetic ($\beta_s < 0$) spin-1 BECs, each component of the ground state is a multiple of one single density function. This is so-called the *single-mode approximation (SMA)* in the literature, which has been justified rigorously in mathematics by Lin and Chern in [20]. As a result, in this case one can compute just one density function instead of three. To show it, we denote $\rho(\mathbf{x}) \geqslant 0$, for $\mathbf{x} \in \mathbb{R}^d$, as a scalar real-valued density function and require it satisfy the normalization condition

$$\|\rho(\cdot)\|^2 = \int_{\mathbb{R}^d} \rho^2(\mathbf{x})\, d\mathbf{x} = 1. \tag{3.5}$$

Let[1] $\Phi_g(\mathbf{x}) = (\phi_{1,g}, \phi_{0,g}, \phi_{-1,g})^T$ be the ground state of a ferromagnetic spin-1 BECs. Based on the single-mode approximation, we can set

$$\phi_{j,g}(\mathbf{x}) = \big|\phi_{j,g}(\mathbf{x})\big| = \gamma_j \rho(\mathbf{x}), \quad \mathbf{x} \in \mathbb{R}^d, \ j = 1, 0, -1 \tag{3.6}$$

with constants $\gamma_j \geqslant 0$ (for $j = 1, 0, -1$). Noticing that the ground state $\Phi_g(\mathbf{x})$ is defined under the constraints of normalization and magnetization described in (3.3), we obtain

$$\gamma_1^2 + \gamma_0^2 + \gamma_{-1}^2 = 1, \qquad \gamma_1^2 - \gamma_{-1}^2 = M. \tag{3.7}$$

Substituting (3.6) into (1.5) and taking (3.7) into account, we obtain

$$E_0(\Phi_g) = \int_{\mathbb{R}^d} \left[\frac{1}{2}\big|\nabla\rho(\mathbf{x})\big|^2 + V_d(\mathbf{x})\rho^2(\mathbf{x}) + \frac{\beta_n}{2}\rho^4(\mathbf{x}) + \frac{\beta_s}{2}\big(M^2 + 2\gamma_0^2(\gamma_1 + \gamma_{-1})^2\big)\rho^4(\mathbf{x})\right] d\mathbf{x}. \tag{3.8}$$

Notice that the minimization of (3.8) over ρ and $(\gamma_1, \gamma_0, \gamma_{-1})$ is separable [20]. Thus, we can take minimization of (3.8) first over $(\gamma_1, \gamma_0, \gamma_{-1})$ and then over ρ. Since $\beta_s < 0$, minimizing (3.8) over $(\gamma_1, \gamma_0, \gamma_{-1})$ is equivalent to

$$\max_{\gamma_1,\gamma_0,\gamma_{-1}} \big\{M^2 + 2\gamma_0^2(\gamma_1 + \gamma_{-1})^2\big\}, \quad \text{subject to (3.7)},$$

which gives the constants

$$\gamma_0 = \sqrt{\frac{1}{2}\big(1 - M^2\big)}, \qquad \gamma_{\pm1} = \frac{1}{2}(1 \pm M). \tag{3.9}$$

Taking (3.9) into account, we define the SMA energy

$$E_{\rm sma}(\rho) := E_0(\Phi_g) = \int_{\mathbb{R}^d} \left[\frac{1}{2}\big|\nabla\rho(\mathbf{x})\big|^2 + V_d(\mathbf{x})\rho^2(\mathbf{x}) + \frac{\kappa}{2}\rho^4(\mathbf{x})\right] d\mathbf{x}, \tag{3.10}$$

where the constant $\kappa = \beta_n + \beta_s$. It is obvious that minimizing $E_0(\Phi_g)$ in (3.8) with constraints (3.3) is equivalent to minimizing $E_{\rm sma}(\rho)$ with the normalization in (3.5) [20].

From the above, we know that for a ferromagnetic system, we can in fact solve for the density function ρ and then obtain the ground state of the corresponding spin-1 BECs by combining (3.6) and (3.9). In detail, we solve the following single-component minimization problem:

[1] For simplicity of notation, in the following sections we will also use $\Phi_g(\mathbf{x})$ to represent the ground state of spin-1 BECs with $B(\mathbf{x}) \equiv 0$. To distinguish it from those when $B(\mathbf{x}) \neq 0$, the readers should refer to the context of the discussion.

Find $(\rho_g(\mathbf{x}) \in S_{\rm sma})$ such that

$$E_{{\rm sma},g} := E_{\rm sma}(\rho_g) = \min_{\rho \in S_{\rm sma}} E_{\rm sma}(\rho) \tag{3.11}$$

over the set

$$S_{\rm sma} = \left\{ \rho(\mathbf{x}) \in \mathbb{R} \,\Big|\, \int_{\mathbb{R}^d} \rho^2(\mathbf{x})\, d\mathbf{x} = 1,\ E_{\rm sma}(\rho) < \infty \right\}.$$

The Euler–Lagrange equation corresponding to (3.11) is given by

$$\mu_{\rm sma}\rho(\mathbf{x}) = -\frac{1}{2}\nabla^2\rho(\mathbf{x}) + V_d(\mathbf{x})\rho(\mathbf{x}) + \kappa\rho^3(\mathbf{x}), \tag{3.12}$$

with the constraint $\|\rho(\cdot)\|^2 = 1$. This is a nonlinear eigenvalue problem with the normalization constraint and the eigenvalue $\mu_{\rm sma}$ can be computed from

$$\mu_{\rm sma}(\rho) = \int_{\mathbb{R}^d} \left[\frac{1}{2}\left|\nabla\rho(\mathbf{x})\right|^2 + V_d(\mathbf{x})\rho^2(\mathbf{x}) + \kappa\rho^4(\mathbf{x}) \right] d\mathbf{x}. \tag{3.13}$$

Similar to that in Section 2, to find the minimizer of (3.11) we solve a gradient flow with discrete normalization and its discretization will be presented for 1D case for simplicity. Generalizations of the method to higher dimensions are straightforward. For $t \in [t_n, t_{n+1}]$, the 1D GFDN corresponding to (3.11) is given by

$$\frac{\partial\rho(x,t)}{\partial t} = \frac{1}{2}\nabla^2\rho - V_1(x)\rho - \kappa\rho^3, \quad x \in [a,b],\ t \in [t_n, t_{n+1}], \tag{3.14}$$

$$\rho\left(x, t_{n+1}^+\right) := \frac{\rho(x, t_{n+1}^-)}{\|\rho(\cdot, t_{n+1}^-)\|}, \quad x \in [a,b], \tag{3.15}$$

where the computational domain $[a,b]$ is chosen to be sufficiently large and homogeneous Dirichlet boundary conditions $\rho(a,t) = \rho(b,t) = 0$ are imposed. At $t = 0$, the initial condition is given by

$$\rho(x,0) = \rho^0(x), \quad x \in [a,b],\ \text{with } \left\|\rho^0(\cdot)\right\| = 1. \tag{3.16}$$

To discretize (3.14)–(3.16), we use the sine pseudo-spectral method for spatial derivatives and the backward/forward Euler scheme for linear/nonlinear terms of the time derivative. The detailed scheme is given as below:

$$\frac{\rho_k^{(1)} - \rho_k^n}{\Delta t} = \frac{1}{2} D_{xx}^s \boldsymbol{\rho}^{(1)}\big|_{x=x_k} - \alpha^n\left(\rho_k^{(1)} - \rho_k^n\right) + F_k^n, \quad k = 1,2,\ldots,K-1, \tag{3.17}$$

$$\rho_k^{n+1} = \frac{\rho_k^{(1)}}{\|\boldsymbol{\rho}^{(1)}\|}, \quad k = 1,2,\ldots,K-1,\ n = 0,1,\ldots, \tag{3.18}$$

where ρ_k^n is the numerical approximation of $\rho(x_k,t_n)$, $\boldsymbol{\rho}^n$ is a vector with components ρ_k^n and $\|\boldsymbol{\rho}^{(1)}\| = \sqrt{\Delta x \sum_{k=1}^{K-1} (\rho_k^{(1)})^2}$. The term

$$F_k^n := F\left(\rho_k^n\right) = -\left[V_1(x_k)\rho_k^n + \kappa\left(\rho_k^n\right)^3\right], \quad k = 1,2,\ldots,K-1,\ n = 0,1,\ldots. \tag{3.19}$$

The operator D_{xx}^s is defined in (2.9). The stabilization parameter $\alpha^n \geqslant 0$ is chosen as [35,5,2]

$$\alpha^n = \frac{1}{2}\Big[\max_{1\leqslant k\leqslant K-1}\left(V_1(x_k) + \kappa\left(\rho_k^n\right)^2\right) + \min_{1\leqslant k\leqslant K-1}\left(V_1(x_k) + \kappa\left(\rho_k^n\right)^2\right)\Big].$$

The initial and boundary conditions are discretized as

$$\rho_k^0 = \rho^0(x_k), \quad k = 0,1,\ldots,K; \qquad \rho_0^n = \rho_K^n = 0, \quad n = 0,1,\ldots, \tag{3.20}$$

respectively. This discrete system can be efficiently solved in the same manner as that for (2.8), (2.11) and (2.12).

3.2. Antiferromagnetic system

In an antiferromagnetic ($\beta_s > 0$) system, the density distribution of atoms in ground states highly depends on the total magnetization M. It was shown in [20] that if $M \neq 0$, the ground states have vanishing zeroth $m_F = 0$ component, i.e., $\phi_{0,g}(\mathbf{x}) \equiv 0$. As a result, the original three-component system is indeed characterized by a two-component reduction. However, if $M = 0$, the ground states of three components satisfy the SMA as given in (3.6). But different from ferromagnetic systems, in this case the constants γ_j are not unique and they are given by $\gamma_1 = \gamma_{-1} = \xi$ and $\gamma_0 = \sqrt{1-2\xi^2}$ for any constant $\xi \in [0, 1/\sqrt{2}]$. For the detailed mathematical proof, we refer the readers to [20]. In the following, we review the two-component reduction and discretize it for computing ground state of antiferromagnetic spin-1 BECs when $B = 0$ and $M \neq 0$. For the case of $M = 0$, the numerical method is identical to that we described in Section 3.1 and thus it is omitted here for brevity.

Let $\Phi_g(\mathbf{x})$ be the ground state of an antiferromagnetic spin-1 BEC with $B = 0$ and $M \neq 0$. Since $\phi_{0,g}(\mathbf{x}) \equiv 0$ in this case, the ground state energy $E_{0,g}$ reduces to

$$E_0(\Phi_g) = \int_{\mathbb{R}^d} \left[\frac{1}{2}\left(|\nabla\phi_{1,g}|^2 + |\nabla\phi_{-1,g}|^2\right) + V_d(\mathbf{x})\left(|\phi_{1,g}|^2 + |\phi_{-1,g}|^2\right) + \frac{\chi}{2}\left(|\phi_{1,g}|^4 + |\phi_{-1,g}|^4\right) + \nu|\phi_{1,g}|^2|\phi_{-1,g}|^2 \right] d\mathbf{x}, \tag{3.21}$$

where the constants $\chi = \beta_n + \beta_s$ and $\nu = \beta_n - \beta_s$. From the constraints of normalization and magnetization in (3.3), it is easy to obtain

$$\int_{\mathbb{R}^d} \left|\phi_{1,g}(\mathbf{x})\right|^2 d\mathbf{x} = \frac{1+M}{2}, \qquad \int_{\mathbb{R}^d} \left|\phi_{-1,g}(\mathbf{x})\right|^2 d\mathbf{x} = \frac{1-M}{2}. \tag{3.22}$$

On the other hand, we define a two-component energy

$$E_{\mathrm{tca}}(u_1, u_2) := \int_{\mathbb{R}^d} \left[\sum_{j=1}^{2} \left(\frac{1}{2}|\nabla u_j|^2 + V_d(\mathbf{x})|u_j|^2 \right) + \frac{\chi}{2}\left(|u_1|^4 + |u_2|^4\right) + \nu|u_1|^2|u_2|^2 \right] d\mathbf{x}. \tag{3.23}$$

It is easy to verify that the ground state $(\phi_{1,g}, \phi_{-1,g})$ minimizes the energy E_{tca} under the constraints (3.22). Hence, the minimization problem defined in (3.1) to find the ground state of an antiferromagnetic spin-1 condensate can be reduced to the following two-component minimization problem:

Find $((u_{1,g}, u_{2,g}) \in S_{\mathrm{tca}})$, such that

$$E_{\mathrm{tca},g} := E_{\mathrm{tca}}(u_{1,g}, u_{2,g}) = \min_{(u_1,u_2)\in S_{\mathrm{tca}}} E_{\mathrm{tca}}(u_1, u_2) \tag{3.24}$$

over the set

$$S_{\mathrm{tca}} = \left\{ (u_1, u_2) \;\middle|\; \|u_1\|^2 = (1+M)/2, \|u_2\|^2 = (1-M)/2, E_{\mathrm{tca}}(u_1, u_2) < \infty \right\}.$$

The ground state of the associated antiferromagnetic spin-1 BECs can be obtained by

$$\phi_{1,g}(\mathbf{x}) = u_{1,g}(\mathbf{x}), \qquad \phi_{0,g}(\mathbf{x}) \equiv 0, \qquad \phi_{-1,g}(\mathbf{x}) = u_{2,g}(\mathbf{x}). \tag{3.25}$$

The Euler–Lagrange equations corresponding to the minimization problem in (3.24) are given by

$$\begin{aligned} \mu_1^{\mathrm{tca}} u_1(\mathbf{x}) &= \left[-\frac{1}{2}\nabla^2 + V_d(\mathbf{x}) + \chi\left|u_1(\mathbf{x})\right|^2 + \nu\left|u_2(\mathbf{x})\right|^2 \right] u_1(\mathbf{x}), \\ \mu_2^{\mathrm{tca}} u_2(\mathbf{x}) &= \left[-\frac{1}{2}\nabla^2 + V_d(\mathbf{x}) + \nu\left|u_1(\mathbf{x})\right|^2 + \chi\left|u_2(\mathbf{x})\right|^2 \right] u_2(\mathbf{x}), \quad \mathbf{x} \in \mathbb{R}^d \end{aligned} \tag{3.26}$$

with the constraints $\|u_1\|^2 = (1+M)/2$ and $\|u_2\|^2 = (1-M)/2$, where the two-component chemical potentials are defined by

$$\mu_j^{\mathrm{tca}} = \int_{\mathbb{R}^d} \left[\frac{1}{2}|\nabla u_j|^2 + V_d(\mathbf{x})|u_j|^2 + \chi|u_j|^4 + \nu|u_j|^2|u_{(3-j)}|^2 \right] d\mathbf{x}, \quad j = 1, 2. \tag{3.27}$$

To find the ground states defined in (3.24), a gradient flow with discrete normalization for two-component system is solved, i.e., over each time interval $[t_n, t_{n+1}]$ (for $n = 0, 1, \ldots$), we solve

$$\frac{\partial u_j(\mathbf{x},t)}{\partial t} = \left[\frac{1}{2}\nabla^2 - V_d(\mathbf{x}) - \chi|u_j|^2 - \nu|u_{(3-j)}|^2\right]u_j(\mathbf{x},t), \quad j=1,2, \tag{3.28}$$

$$u_1(\mathbf{x},t_{n+1}) = \sqrt{\frac{1+M}{2}}\frac{u_1(\mathbf{x},t_{n+1}^-)}{\|u_1(\cdot,t_{n+1}^-)\|}, \qquad u_2(\mathbf{x},t_{n+1}) = \sqrt{\frac{1-M}{2}}\frac{u_2(\mathbf{x},t_{n+1}^-)}{\|u_2(\cdot,t_{n+1}^-)\|}, \tag{3.29}$$

and at time $t=0$, the initial conditions are given by

$$u_j(\mathbf{x},0) = u_j^0(\mathbf{x}), \quad j=1,2 \text{ with } \|u_1^0(\cdot)\| = \sqrt{\frac{1+M}{2}}, \ \|u_2^0(\cdot)\| = \sqrt{\frac{1-M}{2}}. \tag{3.30}$$

In practice, the above gradient flow can be solved in a bounded domain Ω with homogeneous Dirichlet boundary conditions

$$u_1(\mathbf{x},t) = u_2(\mathbf{x},t) = 0, \quad \mathbf{x}\in\partial\Omega, \ t\geqslant 0, \tag{3.31}$$

due to the confinement of the external trapping potentials.

Next we will give the discretization of (3.28)–(3.31) in the 1D case with $\Omega=[a,b]$. Let $u_{j,k}^n$ be the numerical approximation of $u_j(x_k,t_n)$ for $j=1,2$ and $\mathbf{u}_j^n$ be a vector with component $u_{j,k}^n$. Then we have

$$\frac{u_{j,k}^{(1)}-u_{j,k}^n}{\Delta t} = \frac{1}{2}D_{xx}^s\mathbf{u}_j^{(1)}\big|_{x=x_k} - \alpha_j^n\big(u_{j,k}^{(1)}-u_{j,k}^n\big) + G_{j,k}^n, \quad j=1,2, \tag{3.32}$$

$$u_{1,k}^{n+1} = \sqrt{\frac{1+M}{2}}\frac{u_{1,k}^{(1)}}{\|\mathbf{u}_1^{(1)}\|}, \qquad u_{2,k}^{n+1} = \sqrt{\frac{1-M}{2}}\frac{u_{2,k}^{(1)}}{\|\mathbf{u}_2^{(1)}\|}, \quad 1\leqslant k\leqslant K-1, \tag{3.33}$$

where $\|\mathbf{u}_j^{(1)}\| = \sqrt{\Delta x\sum_{k=1}^{K-1}|u_{j,k}^{(1)}|^2}$ for $j=1,2$, and

$$G_{j,k}^n = -\big[V_1(x_k) + \chi\big|u_{j,k}^n\big|^2 + \nu\big|u_{(3-j),k}^n\big|^2\big]u_{j,k}^n, \quad 1\leqslant k\leqslant K-1, \ j=1,2.$$

The stabilization parameters α_j^n $(j=1,2)$ are chosen as

$$\alpha_j^n = \frac{1}{2}\Big[\max_{1\leqslant k\leqslant K-1}\big(V_1(x_k)+\chi\big|u_{j,k}^n\big|^2+\nu\big|u_{(3-j),k}^n\big|^2\big) + \min_{1\leqslant k\leqslant K-1}\big(V_1(x_k)+\chi\big|u_{j,k}^n\big|^2+\nu\big|u_{(3-j),k}^n\big|^2\big)\Big].$$

The operator D_{xx}^s is defined in (2.9). The homogeneous Dirichlet boundary conditions are discretized as

$$u_{1,0}^n = u_{1,K}^n = u_{2,0}^n = u_{2,K}^n = 0, \quad n=0,1,\ldots, \tag{3.34}$$

and the initial conditions are discretized as

$$u_{1,k}^0 = u_1^0(x_k), \qquad u_{2,k}^0 = u_2^0(x_k), \quad k=0,1,\ldots,K. \tag{3.35}$$

For each time step, the discrete system (3.32)–(3.35) can be solved in the same manner as that for (2.8), (2.11) and (2.12).

3.3. Relation between different minimization problems

As we have seen, the ground states of spin-1 BECs are always defined by constrained minimization problems, e.g., (2.1) for $B\neq 0$ and (3.1) for $B\equiv 0$. In the following, we will describe the relation between different minimization problems.

When $B=0$, the ground state can be obtained by minimizing the energy functional E_0 subject to the conservation of both normalization and magnetization. While when $B\neq 0$, the energy E is minimized by requiring only the conservation of normalization. To see the relation between these two minimization problems, we introduce Φ_g^M defined by

Find $(\Phi_g^M\in S^M)$, such that

$$E_g^M := E\big(\Phi_g^M\big) = \min_{\Phi\in S^M} E(\Phi), \tag{3.36}$$

where for a given $M\in[-1,1]$, the set S^M is defined as

$$S^M := \big\{\Phi=(\phi_1,\phi_0,\phi_{-1})^T \ \big| \ \|\Phi(\cdot)\|^2 = 1, \ \|\phi_1(\cdot)\|^2 - \|\phi_{-1}(\cdot)\|^2 = M, \ E(\Phi)<\infty\big\}.$$

That is, Φ_g^M is a minimizer of the energy functional E subject to the conservation of both normalization and magnetization M, where M is a given fixed constant. To obtain the minimizer of the energy E with only the constraint of normalization, one needs to further minimizer E_g^M in (3.36) with respect to $-1\leqslant M\leqslant 1$. Thus, the minimization problem in (2.1) is equivalent to

Find $(\Phi_g\in S)$, such that

$$E(\Phi_g) = \min_{M\in[-1,1]} E\big(\Phi_g^M\big) = \min_{M\in[-1,1]} \min_{\Phi\in S^M} E(\Phi), \tag{3.37}$$

which decomposes (2.1) into two minimization problems. The inner minimization problem is similar to that defined in (3.1) but with different energy functional, while the outer minimization only involves one variable $M \in [-1, 1]$. In the form of (3.37), one can see the effect of the magnetization M on the ground states when $B \neq 0$.

On the other hand, the minimization problem in (3.1) is over three wave functions ϕ_j (for $j = 1, 0, -1$) subject to two constraints. These constraints specify the normalization and total magnetization of the ground states. However, to better understand each component in the ground state, we want to know the norm of individual component. To this end, we define $\Phi_{0,g}^\alpha(\mathbf{x})$ as the minimizer of the following nonconvex minimization problem:

Find $(\Phi_{0,g}^\alpha \in S_0^\alpha)$, such that

$$E_{0,g}^\alpha := E_0\big(\Phi_{0,g}^\alpha\big) = \min_{\Phi\in S_0^\alpha} E_0(\Phi), \tag{3.38}$$

where $\alpha \in [0, 1]$ is a given constant and S_0^α is a nonconvex set defined as

$$S_0^\alpha := \left\{\Phi = (\phi_1, \phi_0, \phi_{-1})^T \;\middle|\; \|\phi_0(\cdot)\|^2 = \alpha,\ \|\phi_{\pm1}(\cdot)\|^2 = \frac{1-\alpha\pm M}{2},\ E_0(\Phi) < \infty\right\}.$$

The minimization problem (3.38) has three unknowns ϕ_j^α $(j = 1, 0, -1)$ and the same number of constraints, which is much easier than the problem in (3.1). In fact, the minimizer $\Phi_{0,g}^\alpha$ can be viewed as a ground state which satisfies the conservation of the total normalization and magnetization as described in (3.3) and also the conservation of the norm for each component.

It is easy to see that to find the ground states $\Phi_{0,g}$ in (3.1), one can first fix α and obtain $\Phi_{0,g}^\alpha$ by minimizing (3.38), and then minimize $E_{0,g}^\alpha$ over $\alpha \in [0, 1]$. Thus, the problem in (3.1) can be decomposed into two minimizing processes, i.e.,

Find $(\Phi_{0,g} \in S_0)$, such that

$$E_0(\Phi_{0,g}) = \min_{\alpha\in[0,1]} E_0\big(\Phi_{0,g}^\alpha\big) = \min_{\alpha\in[0,1]} \min_{\Phi\in S_0^\alpha} E_0(\Phi). \tag{3.39}$$

By minimizing $E_{0,g}^\alpha$ over $0 \leqslant \alpha \leqslant 1$, one can easily obtain the relation between three components in the ground states.

4. Numerical results

In this section, we first test the accuracy of spatial discretization in our numerical methods and then apply them to compute ground states of spin-1 condensates. We remark here that the ground states computed numerically, in general, are independent of time step and time discretization. The ground states are studied when $B(\mathbf{x}) \neq 0$ and some conjectures are made from our numerical observations. In the case of $B(\mathbf{x}) \equiv 0$, we first compare the performance of our methods with those proposed in the literature [6,7,19]. Then we apply our efficient methods to study the ground states of the ferromagnetic and antiferromagnetic spin-1 BECs. In all simulations, the ground states are obtained by setting the tolerance $\varepsilon = 10^{-6}$.

4.1. Numerical accuracy

In order to test the accuracy of the spatial discretization of our methods in different cases, we take $d = 1$, $V_1(x) = x^2/2$ and $\beta_n = 100$ in (1.1) and $M = 0.5$ in (1.7) for the cases when $B = 0$. The ground state is computed on a bounded computational domain chosen as $\Omega = [-32, 32]$. Let Φ_g represent the 'exact' ground state which is obtained numerically by using a very fine mesh $h = \Delta x = 1/64$, and its energy is denoted as $E_{0,g} = E_0(\Phi_g)$ and $E_g = E(\Phi_g)$ when $B(\mathbf{x}) = 0$ and $B(\mathbf{x}) \neq 0$, respectively. Similarly, let Φ_g^h be the ground states computed by using the mesh size h and its energy is denoted as $E_{0,g}^h = E_0(\Phi_g^h)$ and $E_g^h = E(\Phi_g^h)$ when $B(\mathbf{x}) = 0$ and $B(\mathbf{x}) \neq 0$, respectively. Table 1 lists the errors in terms of the ground state, i.e., $\|\Phi_g - \Phi_g^h\|$, and the ground state energy, i.e., $|E_{0,g} - E_{0,g}^h|$ or $|E_g - E_g^h|$, under different mesh size h for three different cases: (i) ferromagnetic case with $B = 0$ and $\beta_s = -10\sqrt{2}$; (ii) antiferromagnetic case with $B = 0$ and $\beta_s = 10\sqrt{2}$; and (iii) nonzero external magnetic field with $B = 1 + 2i$ and $\beta_s = -10\sqrt{2}$.

From Table 1 and additional results not shown here for brevity, it is easy to see that our numerical methods are spectral order accurate in space for computing the ground states and its energy. Therefore when the solution changes rapidly with optical lattice potential and/or high accuracy is required, in general, our methods need much less grid points than those low-order finite difference or finite element methods, and thus the memory cost and/or computational cost will be saved significantly, especially in 2D and 3D.

4.2. Numerical results for $B \neq 0$

In the following, we study ground states of spin-1 BECs when $B(\mathbf{x}) \neq 0$. We start with 1D condensates and both the ferromagnetic and antiferromagnetic systems are considered. Then the ground states of 2D spin-1 BECs are studied for different Ioffe–Pritchard magnetic field B.

Table 1
Spatial accuracy analysis of our methods for computing ground states of spin-1 BECs under different cases.

Mesh size	$B=0,\ \beta_s=-10\sqrt{2}$		$B=0,\ \beta_s=10\sqrt{2}$		$B=1+2i,\ \beta_s=-10\sqrt{2}$	
	$\|\Phi_g-\Phi_g^h\|$	$\|E_{0,g}-E_{0,g}^h\|$	$\|\Phi_g-\Phi_g^h\|$	$\|E_{0,g}-E_{0,g}^h\|$	$\|\Phi_g-\Phi_g^h\|$	$\|E_g-E_g^h\|$
$h=2$	6.4057E-3	1.3476E-2	1.5939E-2	2.6943E-2	7.0229E-3	6.9005E-3
$h=1$	1.7707E-3	5.5643E-4	2.2937E-3	3.9818E-6	2.6652E-3	1.1460E-3
$h=1/2$	2.7409E-5	6.7342E-7	3.4688E-5	9.5812E-7	2.9747E-5	4.7819E-6
$h=1/4$	2.7159E-9	5.6843E-14	3.7193E-8	2.5224E-13	7.8498E-8	6.9473E-8

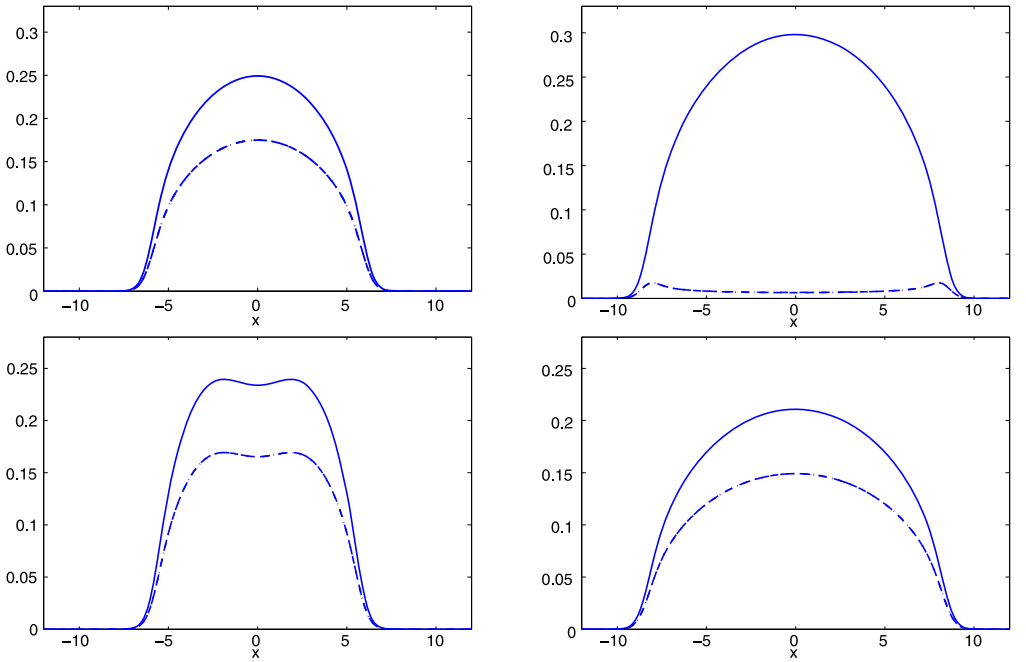

Fig. 1. Ground states of spin-1 BECs in ferromagnetic (left) and antiferromagnetic (right) systems, where $B(x)=\cos(x)+i\cos(x)$ (top) and $B(x)=\cos(x)+i\sin(x)$ (bottom). Dash line: $|\phi_{1,g}|$; solid line: $|\phi_{0,g}|$; dash-dot line: $|\phi_{-1,g}|$. Notice that the graphs of $|\phi_{1,g}|$ and $|\phi_{-1,g}|$ are identical.

Example 1. We study ground states of 1D spin-1 condensates confined in a harmonic potential $V_1(x)=x^2/2$. In our simulations, we choose computational domain $[-32,32]$, mesh size $\Delta x=0.03125$ and time step $\Delta t=0.001$. The parameters $\beta_n=400$, and $\beta_s=\mp 250$ for ferromagnetic and antiferromagnetic cases, respectively. Then we study the following two cases:

Case I. $B(x)\in\mathbb{C}$ is a periodic function of $x\in\mathbb{R}$. Fig. 1 shows the ground states in both ferromagnetic and antiferromagnetic systems, where $B(x)=\cos(x)+i\cos(x)$ or $B(x)=\cos(x)+i\sin(x)$. We see that the density functions of ground states are always symmetric with respect to $x=0$ which is the center of external trap $V_1(x)$. In addition, the $m_F=\pm 1$ components have the same density, which implies that when $B(x)$ is nonzero, the stationary states with total magnetization $M=0$ have the lowest energy.

Case II. $B(x)\equiv B\in\mathbb{C}$ is a constant. Fig. 2 shows the ground states for the constant field $B=3+4i$. From it and our extensive simulations (not shown here for brevity), we find that when $B(x)$ is a constant, the ground states satisfy exactly the single-mode approximation defined in (3.6), which is independent of ferromagnetic or antiferromagnetic characterizations. Furthermore, our numerical results suggest that here (i) the SMA constants are $\gamma_1=\gamma_{-1}=\frac{1}{2}$ and $\gamma_0=\frac{\sqrt{2}}{2}$; (ii) the SMA density function depends only on interaction parameters β_n and β_s but not on constant B; (iii) the SMA ground state energy depends on the modules of B, i.e., $|B|$, instead of B.

To further study the SMA energies in Case II, we compute the ground states with respect to different parameters β_n, β_s and B. Figs. 3–4 present the ground state energy for ferromagnetic and antiferromagnetic cases, respectively. We see that if the constant $|B|$ is fixed, the larger the constant $\beta_n+\beta_s$, the higher the ground state energy, which holds for both ferromagnetic (cf. Fig. 3 left) and antiferromagnetic (cf. Fig. 4 left) cases. On the other hand, for fixed $\beta_n+\beta_s$, the ground state energy depends on $|B|$ instead of B; see Fig. 3 right and Fig. 4 right for ferromagnetic and antiferromagnetic cases, respectively, where real-valued constants B are chosen. For fixed $\beta_n+\beta_s$, the energy in ferromagnetic system linearly

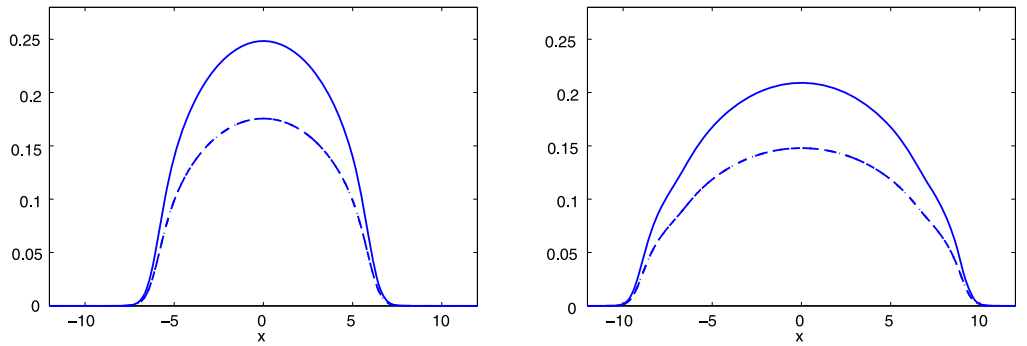

Fig. 2. Ground states of spin-1 BECs in ferromagnetic (left) and antiferromagnetic (right) systems, where $B(x) \equiv B = 3 + 4i$. Dash line: $|\phi_{1,g}|$; solid line: $|\phi_{0,g}|$; dash-dot line: $|\phi_{-1,g}|$. Notice that the graphs of $|\phi_{1,g}|$ and $|\phi_{-1,g}|$ are identical.

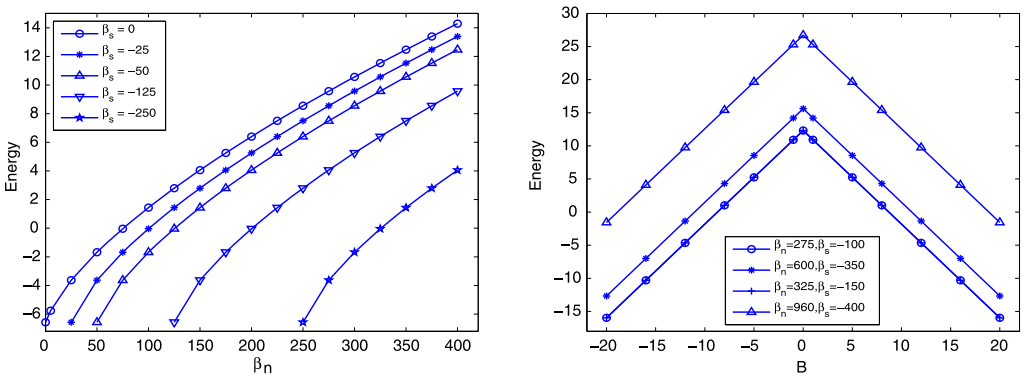

Fig. 3. Energy versus the interaction parameter β_n with $|B| = 5$ fixed (left) and versus the constant B (right) in ferromagnetic cases.

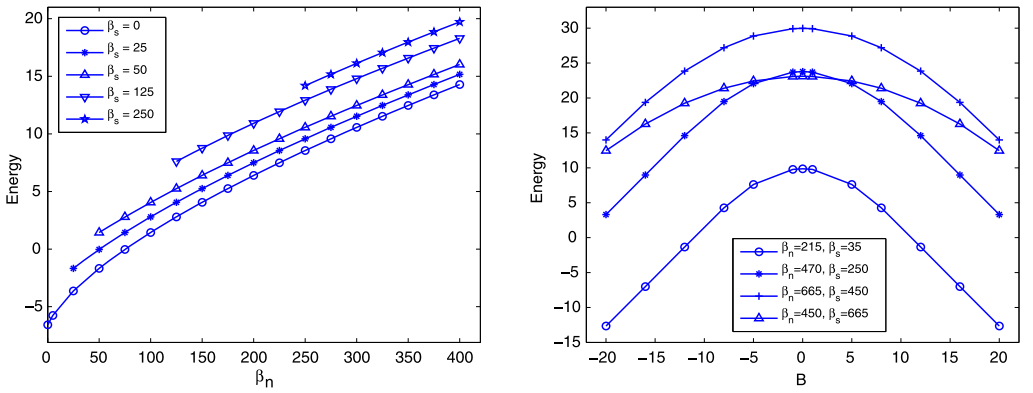

Fig. 4. Energy versus the interaction parameter β_n with $|B| = 5$ fixed (left) and versus the real-valued constant B (right) in antiferromagnetic cases.

depends on $|B|$. However, in antiferromagnetic case, the same constants $\beta_n + \beta_s$ and $|B|$ may result in different ground state energy (cf. Fig. 4 right).

Example 2. We study ground states of 2D spin-1 BECs in an isotropic harmonic potential $V_2(\mathbf{x}) = (x^2 + y^2)/2$. Figs. 5–7 show the density functions of the ground states for $B(x, y) = \sin(x) + \sin(y)$, $\sin(x) + i\sin(y)$ and $1 + 2i$, respectively. Similar to the 1D case, the densities of $m_F = \pm 1$ components are identical, which is true for both ferromagnetic and antiferromagnetic condensates. Furthermore, if the complex-valued $B(x, y)$ is space-dependent, then quantum vortices appear in the ground states; see Fig. 6. However, if $B(x, y) \equiv B$ is a constant, no vortex is observed; furthermore, the ground states in this case satisfy the SMA and the SMA constants γ_j are always $\gamma_{\pm 1} = \frac{1}{2}$ and $\gamma_0 = \frac{\sqrt{2}}{2}$ for any constant B.

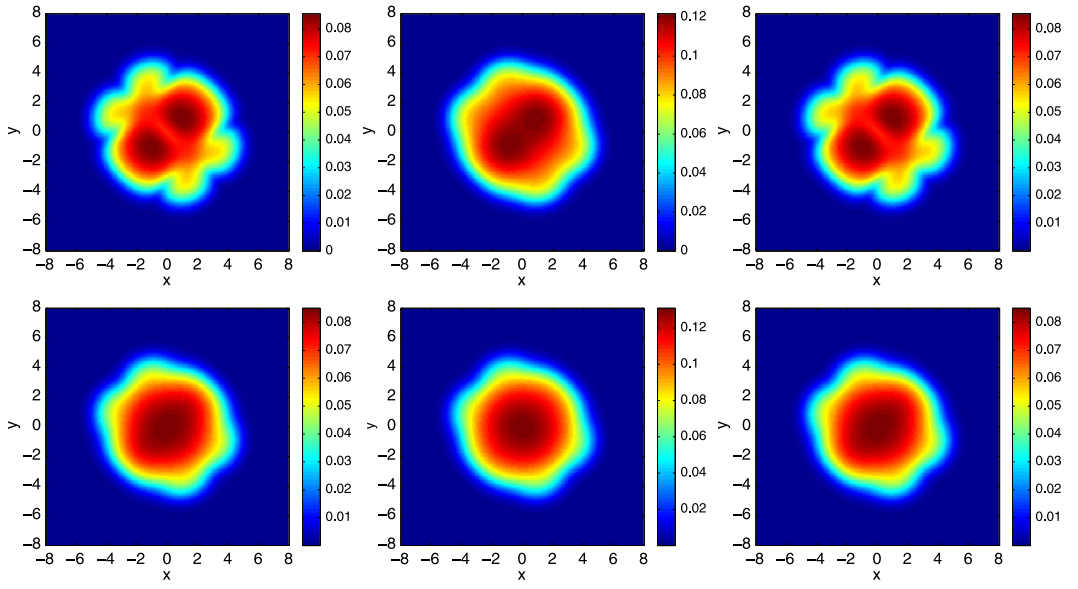

Fig. 5. Ground states of ferromagnetic (top) and antiferromagnetic (bottom) spin-1 BECs with $B(x, y) = \sin(x) + \sin(y)$. From left to right: $|\phi_{1,g}|$, $|\phi_{0,g}|$ and $|\phi_{-1,g}|$.

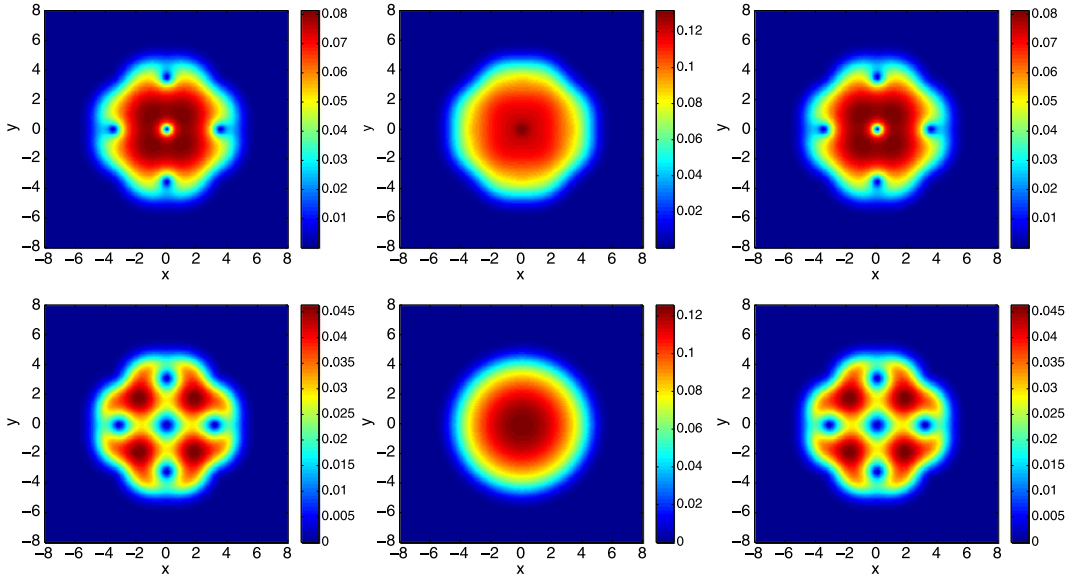

Fig. 6. Ground states of ferromagnetic (top) and antiferromagnetic (bottom) spin-1 BECs with $B(x, y) = \sin(x) + i\sin(y)$. From left to right: $|\phi_{1,g}|$, $|\phi_{0,g}|$ and $|\phi_{-1,g}|$.

4.3. Numerical results for $B = 0$

Next, we first compare our methods in Section 3 with those proposed in the literature [6,7,19,10]. Then we apply our methods to study ground states in ferromagnetic and antiferromagnetic systems when $B(\mathbf{x}) = 0$.

4.3.1. Comparison of different methods

Numerical methods presented in [6,7,19,10] for computing ground states of spin-1 BECs are computationally intensive because they solve a coupled three-component system. However, our methods introduced in Section 3 take into account the ferromagnetic or antiferromagnetic characterizations of the corresponding ground states and thus provide more efficient approaches for simulating the ground states in the case of $B(\mathbf{x}) \equiv 0$. To show the effectiveness of our methods, we compare them with that proposed in [7], which we will refer to as Bao–Lim's method for simplicity. We remark here that it has been pointed out in [7] that Bao–Lim's method is more efficient than other methods proposed for computing ground states

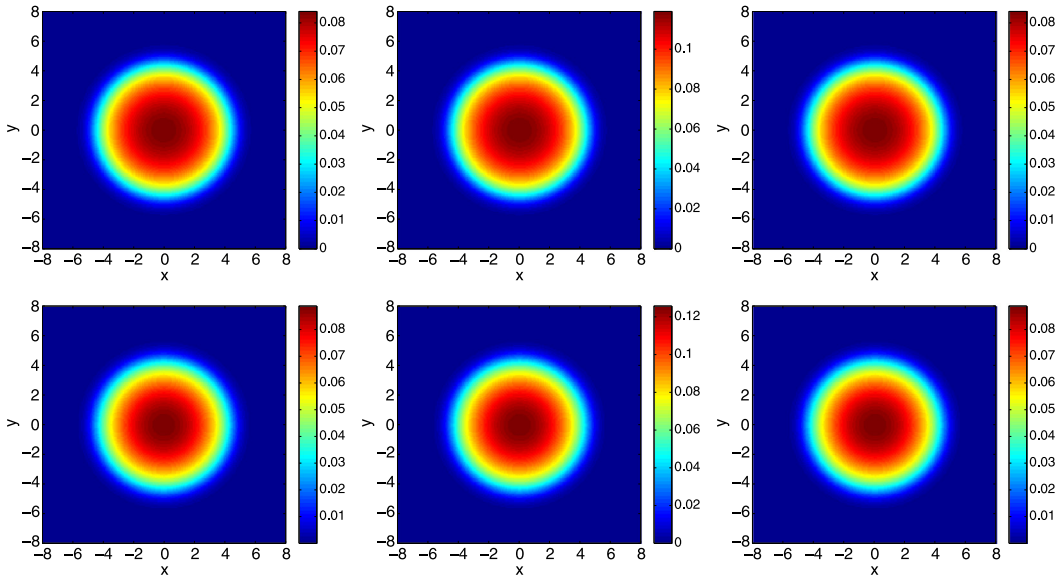

Fig. 7. Ground states of ferromagnetic (top) and antiferromagnetic (bottom) spin-1 BECs with $B(x, y) = 1 + 2i$. From left to right: $|\phi_{1,g}|$, $|\phi_{0,g}|$ and $|\phi_{-1,g}|$.

Table 2
Ground state energy and computing time (i.e., CPU time in seconds) by Bao–Lim's method [7] and our method in Section 3.1 for ferromagnetic condensates with different magnetizations $0 \leqslant M \leqslant 1$.

M	Bao–Lim's method (in seconds)	Our method (in seconds)
0	132.90	6.65
0.1	145.18	6.65
0.2	223.50	6.65
0.3	271.15	6.65
0.4	288.82	6.65
0.5	282.16	6.65
0.6	259.82	6.65
0.7	239.03	6.65
0.8	166.89	6.65
0.9	119.05	6.65
Energy	$E_0(\Phi_g) = 35.4007$	$E_{\text{sma}}(u_g) = 35.4007$

of spin-1 BECs in the literature, and hence in the following we will only compare our method with Bao–Lim's method. Different methods are compared in terms of the ground state energy and the computing time.

In the following, we consider 1D cases, i.e., $d = 1$, and the external potential is chosen as $V_1(x) = x^2/2$. The problem is solved in a computational domain $[-32, 32]$ with $K = 2048$, i.e., the mesh size $\Delta x = 0.03125$. The time step is $\Delta t = 0.001$ in our simulations. We denote N as the total number of atoms and choose $N = 10\,000$ in the following examples. Since in ground states we have $M \leftrightarrow -M \Leftrightarrow \phi_1 \leftrightarrow \phi_{-1}$, here we will only present the results for $0 \leqslant M \leqslant 1$.

Example 3. We consider a ferromagnetic spin-1 condensate with $\beta_n = 0.08716N$ and $\beta_s = -0.001748N$. The values of the interaction parameters β_n and β_s correspond to the experimental setup of ^{87}Rb confined in a cigar-shaped trapping potential with parameters used in [24,25,29]. Correspondingly, the constant κ in the SMA formulation (3.10) is $\kappa = 0.085412N$.

For different magnetization $0 \leqslant M \leqslant 1$, we compare the ground states computed by our method based on the single-mode approximation in (3.6) and (3.9) and by Bao–Lim's method [7]. Fig. 8 shows the density of each component in the ground states. Table 2 shows the ground state energy and computing time (in seconds) used by different methods. Note that here our motivation is to compare the speed of two methods in computing the ground states, and the programs by different methods are run on the same computer. We understand that the computing time can be shortened if one uses an advanced computer or does parallel computations, which however is beyond our interest here.

It shows in Fig. 8 that the ground states computed by our method are consistent with those by Bao–Lim's method for different magnetization M, where lines represent the results by our method and symbols represent those from Bao–Lim's method [7]. From Table 2, we see that the ground state energies obtained from both methods are the same; furthermore, in this case the energy is independent of magnetization M. However, the computing time used by our method is much shorter (less than 6%) than that of Bao–Lim's method [7]. In addition, the computing time by Bao–Lim's method [7] depends variously on the magnetization M.

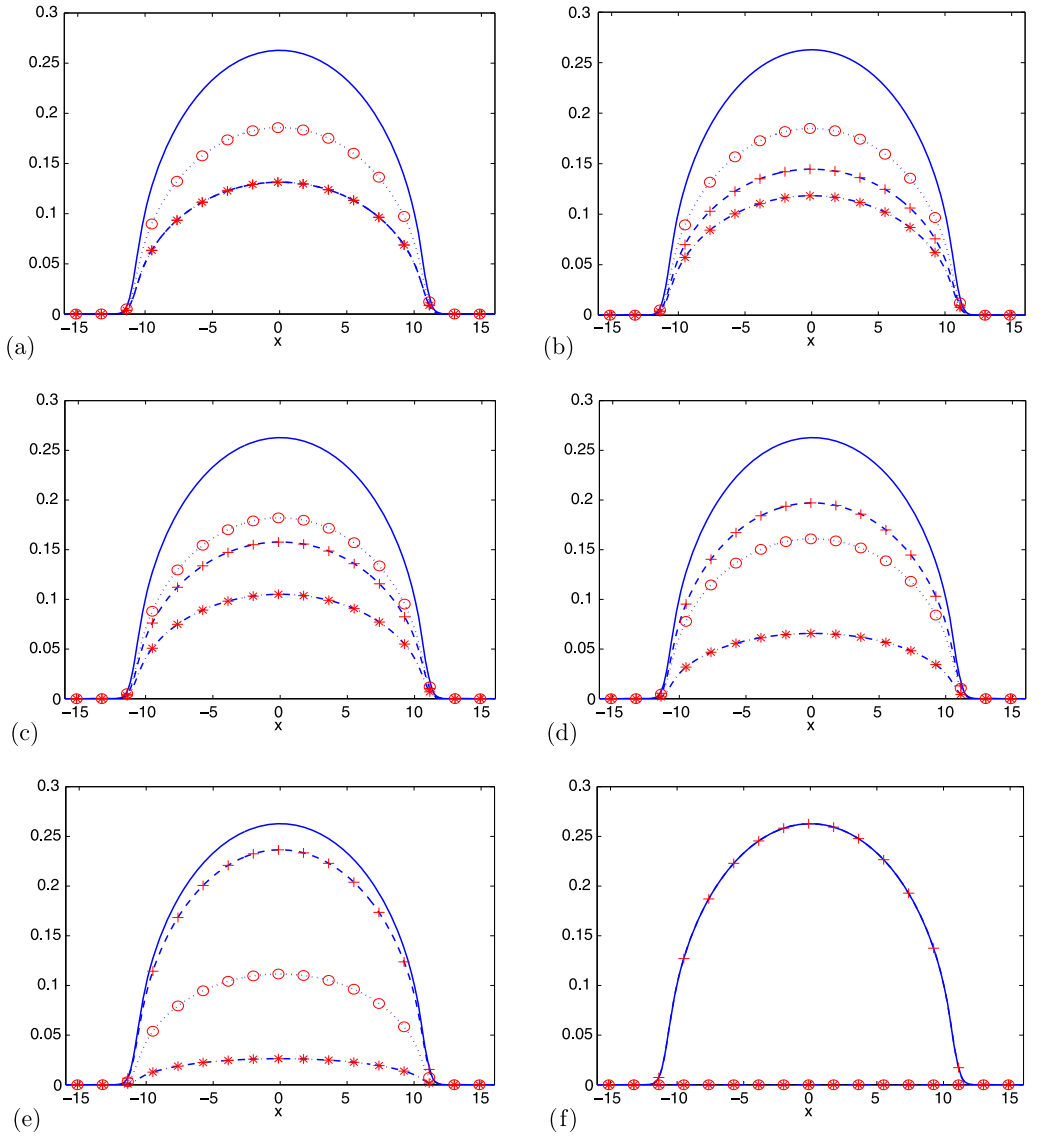

Fig. 8. Ground states of the ferromagnetic spin-1 BECs in Example 3 computed by Bao–Lim's method ('+': $|\phi_{1,g}|$, 'o': $|\phi_{0,g}|$; '*': $|\phi_{-1,g}|$) and our method based on SMA (solid line: $u_g(x)$; dash line: $|\phi_{1,g}| = \gamma_1 u_g$; dot line: $|\phi_{0,g}| = \gamma_0 u_g$; dash-dot line: $|\phi_{-1,g}| = \gamma_{-1} u_g$ with γ_j given in (3.9)). From (a) to (f): $M = 0, 0.1, 0.2, 0.5, 0.8, 1$.

Example 4. We consider an antiferromagnetic spin-1 condensate with $\beta_n = 0.0241N$ and $\beta_s = 0.00075N$ in (1.1), which corresponds to $\chi = 0.02485N$ and $\nu = 0.02335N$ in the two-component reduction when $M \neq 0$. The values of these parameters correspond to the experimental setup of ^{23}Na confined in a cigar-shaped trapping potential with parameters used in [24,25,29].

Similarly, we compare the ground states computed by these two methods in Fig. 9 and the ground state energies and computing time (in seconds) for different magnetization $0 \leqslant M \leqslant 1$ are listed in Table 3. We see that for a fixed magnetization $M \neq 0$, the two methods obtain the identical ground states with $\phi_{0,g}(x) \equiv 0$. In addition, the ground state energy is also the same. However, Table 2 suggests that our method based on the two-component reduction is much faster than Bao–Lim's method [7] which solves a three-component system. Furthermore, even though our method solves a two-component GFDN, its computing time is much less (between 10% and 50%) than that used by Bao–Lim's method. We remark again that our motivation here is to compare the speed of these two methods. For this purpose, we run the programs of both methods on the same computer and their computing time might be reduced if an advanced computer is used.

The above one-dimensional examples have shown that our methods based on the ferromagnetic and antiferromagnetic characterization are much faster than Bao–Lim's method. For problems in 2D and 3D, the saving in the computational time is much more apparent. For example, the computational time used by Bao–Lim's method in 2D or 3D cases can different from severals hours to days, but our methods usually take several minutes or hours.

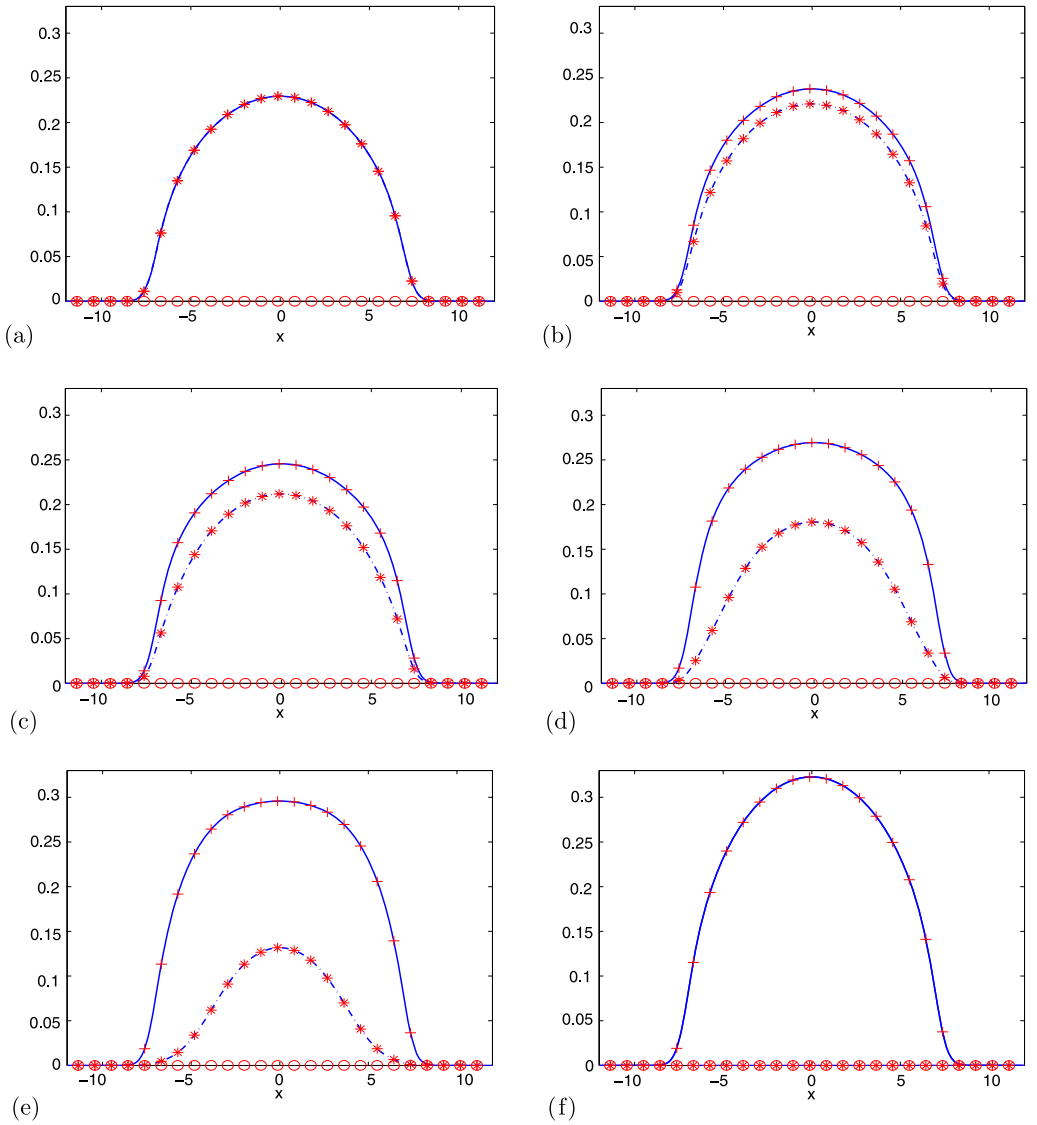

Fig. 9. Ground states of the antiferromagnetic spin-1 BECs in Example 4 computed by Bao–Lim's method ('+': $|\phi_{1,g}|$, 'o': $|\phi_{0,g}|$; '*': $|\phi_{-1,g}|$) and our method based on the two-component reduction (solid line: $|\phi_{1,g}| = |u_{1,g}|$; dot line: $|\phi_{0,g}|$; dash-dot line: $|\phi_{-1,g}| = |u_{2,g}|$). From (a) to (f): $M = 0, 0.1, 0.2, 0.5, 0.8, 1$.

4.3.2. Applications of our methods

In Section 4.3.1, we showed that our methods, based on the ferromagnetic or antiferromagnetic characterization of spin-1 BECs, obtain the same ground states as those by Bao–Lim's method [7]. However, the computing time consumed by our methods is much less, which makes them more efficient in computing the ground states of spin-1 condensates when $B(\mathbf{x}) = 0$. In the following, we will apply our methods to study the ground states in different cases.

Example 5. We test the dependence of ground state energies on the interaction parameters β_n and β_s as well as on the magnetization M. To do this, 1D spin-1 BECs with a harmonic external potential $V_1(x) = x^2/2$ are considered. The computational domain is $[-32, 32]$ which is sufficiently large so that the truncation errors can be neglected. We choose the mesh size and time step as $\Delta x = 0.03125$ and $\Delta t = 0.001$, respectively. Then we consider the following two cases:

Case I. Ferromagnetic system with $\beta_s < 0$. Fig. 10 (top) shows the ground state energy with respect to different interaction constants β_n and β_s and different magnetization M. It suggests that the energy monotonically increases with $\beta_n + \beta_s$ increasing, but it is independent of the magnetization M. Furthermore when $\beta_n + \beta_s$ is large, the ground state energy of a ferromagnetic spin-1 condensate can be approximated by the Thomas–Fermi energy of its SMA counterpart, i.e.,

Table 3
Ground state energy and computing time (i.e., CPU time in seconds) by Bao–Lim's method [7] and our method in Section 3.2 for antiferromagnetic condensates with different magnetization $0 \leqslant M \leqslant 1$.

M	Bao–Lim's method		Our method	
	Energy $E_0(\Phi_g)$	Computing time (in seconds)	Energy $E_{\rm tca}(\mathbf{u}_g)$	Computing time (in seconds)
0	15.2485	177.1892	15.2485	15.1419
0.1	15.2513	177.0494	15.2513	42.0558
0.2	15.2599	176.9190	15.2599	47.3362
0.3	15.2743	176.8998	15.2743	51.9579
0.4	15.2945	176.2563	15.2945	56.6422
0.5	15.3209	174.9268	15.3209	61.6046
0.6	15.3537	172.9923	15.3537	66.4197
0.7	15.3933	168.8066	15.3933	70.8586
0.8	15.4405	163.0863	15.4405	74.9606
0.9	15.4962	158.1879	15.4962	79.2583

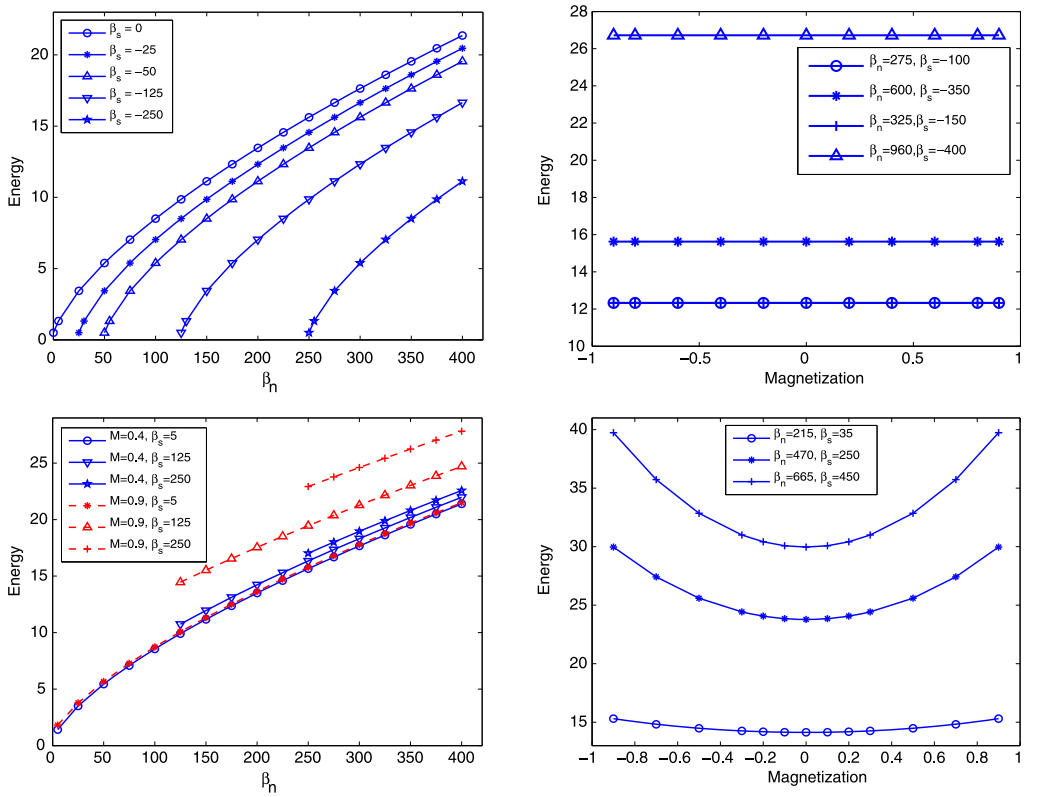

Fig. 10. Energy versus the interaction constants β_n and β_s (left) and the magnetization M (right) in ferromagnetic (top) and antiferromagnetic (bottom) spin-1 condensates.

$$E_{0,g} \approx E^{\rm TF}_{{\rm sma},g} = \frac{3}{10}\left(\frac{3\kappa\gamma_x}{2}\right)^{\frac{2}{3}}, \tag{4.1}$$

where γ_x is the trapping frequency in x-direction and in this example, we use $\gamma_x = 1$.

Case II. Antiferromagnetic system with $\beta_s > 0$. Fig. 10 (bottom) shows the ground state energy for different parameters β_n, β_s and M. Different from that in ferromagnetic cases, the ground state energy in an antiferromagnetic system depends on the constants $\beta_n + \beta_s$, $\beta_n - \beta_s$ and the magnetization M. For fixed $\beta_n \pm \beta_s$, the ground state energy increases when the magnitude of M, i.e., $|M|$, increases, and the energy reaches its minimizer at $M = 0$; see Fig. 10 (bottom, right).

Example 6. We apply our methods to study ground states of 2D spin-1 condensates. The following two types of external potentials are considered: (i) harmonic potential $V_2(\mathbf{x}) = (\gamma_x^2 x^2 + \gamma_y^2 y^2)/2$; (ii) isotropic harmonic potential plus an optical lattice, i.e.,

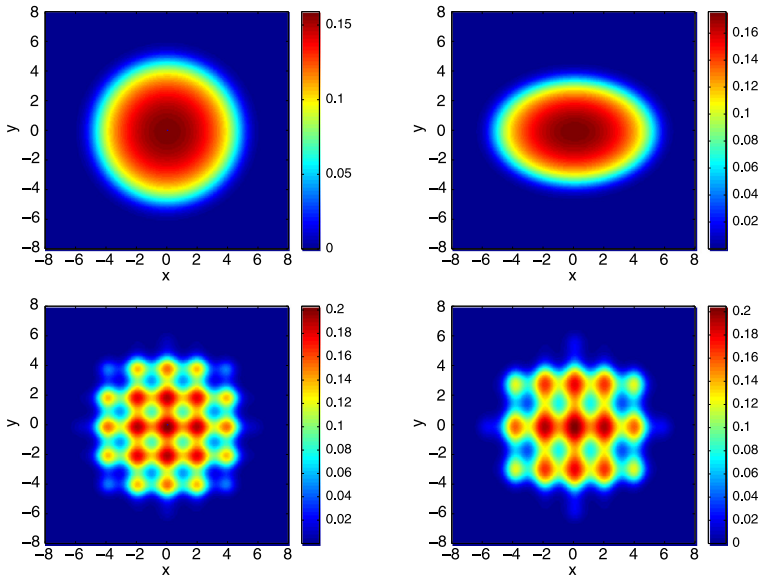

Fig. 11. Ground states of 2D ferromagnetic spin-1 BECs in Example 6 with a harmonic trap (top: $\gamma_x = \gamma_y = 1$ (left); $\gamma_x = 1$ and $\gamma_y = 1.5$ (right)) and a harmonic plus optical lattice potential (bottom: $\kappa_x = \kappa_y = \frac{\pi}{2}$ (left); $\kappa_x = \frac{\pi}{2}$ and $\kappa_y = \frac{\pi}{3}$ (right)).

$$V_2(\mathbf{x}) = \frac{1}{2}\left(x^2 + y^2\right) + 10\left[\sin^2(\kappa_x x) + \sin^2(\kappa_y y)\right], \tag{4.2}$$

where $\kappa_x, \kappa_y > 0$ are two constants. Then we study the ground states of

Case I. Ferromagnetic system with $\beta_n = 560$ and $\beta_s = -100$ and $M = 0.5$.

Case II. Antiferromagnetic system with $\beta_n = 300$, $\beta_s = 100$ and $M = 0.5$.

Fig. 11 presents the density of ground states calculated from the single-mode reduction for ferromagnetic cases, and the ground states of the corresponding spin-1 BECs can be obtained by using (3.6) and (3.9) with $M = 0.5$. Fig. 12 shows the ground states of antiferromagnetic spin-1 condensates, where only $|\phi_{1,g}| = |u_{1,g}|$ and $|\phi_{-1,g}| = |u_{2,g}|$ are presented since $|\phi_{0,g}| \equiv 0$ in this case. Numerical simulations show that our methods based on the single-mode and two-component reduction are dramatically faster than the Bao–Lim's method [7] in higher dimensional cases.

5. Conclusions

We proposed efficient and simpler numerical methods for computing ground states of spin-1 BEC with/without the Ioffe–Pritchard magnetic field $B(\mathbf{x})$. Noticing that there have been no numerical studies on the ground state of spin-1 BECs with $B(\mathbf{x}) \neq 0$, we first introduced a numerical method for it. Then our methods were applied to study the ground states in both 1D and 2D cases. Our numerical results suggested that when $B(\mathbf{x}) \neq 0$, the $m_F = \pm 1$ components in the ground states always have the same density functions, which implies that the stationary states with the magnetization $M = 0$ have the minimum energy. In particular, if $B(\mathbf{x}) \equiv B \neq 0$ is a constant, the ground states satisfy the single-mode reduction given in (3.6) with the constants $\gamma_{\pm 1} = \frac{1}{2}$ and $\gamma_0 = \frac{\sqrt{2}}{2}$ exactly. We will leave its rigorous mathematical justifications for future work.

On the other hand, when $B(\mathbf{x}) = 0$, we took into account the ferromagnetic or antiferromagnetic characterizations of the ground states [20], which results in efficient numerical methods for computing the ground state. In the ferromagnetic cases, the ground state can be always described exactly by the single-mode approximation. While in the antiferromagnetic systems, the situations can be classified into two types: (i) when $M \neq 0$, the $m_F = 0$ component becomes zero in the ground states so that the spin-1 BECs can be characterized by a two-component reduction; (ii) if $M = 0$, the ground states satisfy the SMA as in the ferromagnetic systems, but the constants are not unique. Considering these properties of the ground states, we proposed numerical methods to compute the ground state of the reduced single-mode or two-component systems. Then the ground states of the original spin-1 condensates can be obtained from those of the reduced systems. Numerical results suggested that our methods give the same results as those by Bao–Lim's method in [7,19]. However, the computing time used by our methods is much shorter and the implementation is much easier and simpler. In addition, we apply our methods to study the relation between the ground state energy and the interaction parameters β_n, β_s as well as the magnetization M.

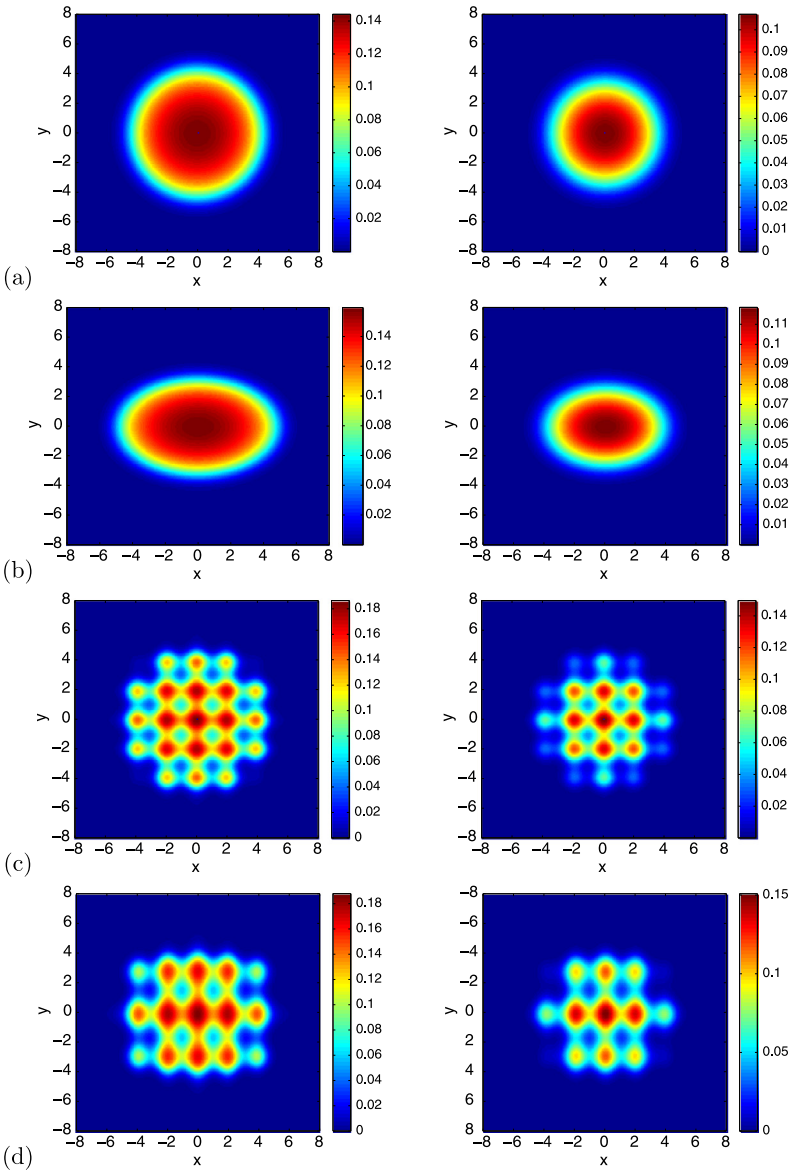

Fig. 12. Ground states of 2D antiferromagnetic spin-1 BECs in Example 6 with a harmonic trap (top: $\gamma_x = \gamma_y = 1$ (a); $\gamma_x = 1$ and $\gamma_y = 1.5$ (b)) and a harmonic plus optical lattice potential (bottom: $\kappa_x = \kappa_y = \frac{\pi}{2}$ (c); $\kappa_x = \frac{\pi}{2}$ and $\kappa_y = \frac{\pi}{3}$ (d)).

Acknowledgement

This work was supported by the Singapore A*STAR SERC PSF-Grant 1321202067 (W. Bao), the National Science Council of the Republic of China Grant 99-2115-M-002-003-MY3 (I-L. Chern), and the University of Missouri Research Board and the Simons Foundation Award No. 210138 (Y. Zhang). Part of this work was done when the authors were visiting the Institute for Mathematical Sciences at the National University of Singapore in 2012.

References

[1] M.H. Anderson, J.R. Ensher, M.R. Matthews, C.E. Wieman, E.A. Cornell, Observation of Bose–Einstein condensation in a dilute atomic vapor, Science 269 (1995) 198–201.
[2] W. Bao, Y. Cai, Mathematical theory and numerical methods for Bose–Einstein condensation, Kinet. Relat. Mod. 6 (2013) 1–135.
[3] W. Bao, Q. Du, Computing the ground state solution of Bose–Einstein condensates by a normalized gradient flow, SIAM J. Sci. Comput. 25 (2004) 1674–1697.
[4] W. Bao, Q. Du, Y. Zhang, Dynamics of rotating Bose–Einstein condensates and their efficient and accurate numerical computation, SIAM J. Appl. Math. 66 (2006) 758–786.

[5] W. Bao, I-L. Chern, F.Y. Lim, Efficient and spectrally accurate numerical methods for computing ground and first excited states in Bose–Einstein condensates, J. Comput. Phys. 219 (2006) 836–854.
[6] W. Bao, H. Wang, A mass and magnetization conservative and energy-diminishing numerical method for computing ground state of spin-1 Bose–Einstein condensates, SIAM J. Numer. Anal. 45 (2007) 2177–2200.
[7] W. Bao, F.Y. Lim, Computing ground states of spin-1 Bose–Einstein condensates by the normalized gradient flow, SIAM J. Sci. Comput. 30 (2008) 1925–1948.
[8] W. Bao, Y. Zhang, Dynamical laws of the coupled Gross–Pitaevskii equations for spin-1 Bose–Einstein condensates, Meth. Appl. Anal. 17 (2010) 49–80.
[9] D. Cao, I-L. Chern, J.-C. Wei, On ground states of spinor Bose–Einstein condensates, Nonlinear Differ. Equ. Appl. 18 (2011) 427–445.
[10] J.-H. Chen, I-L. Chern, W. Wang, Exploring ground states and excited states of spin-1 Bose–Einstein condensates by continuation methods, J. Comput. Phys. 230 (2011) 2222–2236.
[11] M.L. Chiofalo, S. Succi, M.P. Tosi, Ground state of trapped interacting Bose–Einstein condensates by an explicit imaginary-time algorithm, Phys. Rev. E 62 (2002) 7438–7444.
[12] K.B. Davis, M.O. Mewes, M.R. Andrews, N.J. van Druten, D.S. Durfee, D.M. Kurn, W. Ketterle, Bose–Einstein condensation in a gas of sodium atoms, Phys. Rev. Lett. 75 (1995) 3969–3973.
[13] U. Ernst, A. Marte, F. Schreck, J. Schuster, G. Rempe, Bose–Einstein condensation in a pure Ioffe–Pritchard field configuration, Europhys. Lett. 41 (1998) 1–6.
[14] T.L. Ho, Spinor Bose condensates in optical traps, Phys. Rev. Lett. 81 (1998) 742–745.
[15] T.-L. Ho, S.K. Yip, Fragmented and single condensate ground states of spin-1 Bose gas, Phys. Rev. Lett. 84 (2000) 4031–4034.
[16] T. Isoshima, M. Nakahara, T. Ohmi, K. Machida, Creation of a persistent current and vortex in a Bose–Einstein condensate of alkali-metal atoms, Phys. Rev. A 61 (2000), article 063610.
[17] C.K. Law, H. Pu, N.P. Bigelow, Quantum spins mixing in spinor Bose–Einstein condensates, Phys. Rev. Lett. 81 (1998) 5257–5261.
[18] A.E. Leanhardt, Y. Shin, D. Kielpinski, D.E. Pritchard, W. Ketterle, Coreless vortex formation in a spinor Bose–Einstein condensate 90 (2003), article 140403.
[19] F.Y. Lim, W. Bao, Numerical methods for computing the ground state of spin-1 Bose–Einstein condensates in a uniform magnetic field, Phys. Rev. E 78 (2008), article 066704.
[20] L. Lin, I-L. Chern, Proofs of some simplified characterizations of the ground states of spin-1 Bose–Einstein condensates, arXiv:1102.0832v3.
[21] L. Lin, I-L. Chern, Bifurcation between 2-component and 3-component ground states of spin-1 Bose–Einstein condensates in uniform magnetic fields, arXiv:1302.0279.
[22] M. Matuszewski, T.J. Alexander, Y.S. Kivshar, Excited spin states and phase separation in spinor Bose–Einstein condensates, Phys. Rev. A 80 (2009), article 023602.
[23] M. Matuszewski, Ground states of trapped spin-1 condensates in magnetic field, Phys. Rev. A 82 (2010), article 053630.
[24] H.-J. Miesner, D.M. Stamper-Kurn, J. Stenger, S. Inouye, A.P. Chirkkatur, W. Ketterle, Observation of metastable states in spinor Bose–Einstein condensates, Phys. Rev. Lett. 82 (1999) 2228–2231.
[25] T. Mizushima, N. Kobayashi, K. Machida, Coreless and singular vortex lattices in rotating spinor Bose–Einstein condensates, Phys. Rev. A 70 (2004), article 043613.
[26] K. Murata, H. Saito, M. Ueda, Broken-axisymmetry phase of a spin-1 ferromagnetic Bose–Einstein condensate, Phys. Rev. A 75 (2007), article 013607.
[27] T. Ohmi, K. Machida, Bose–Einstein condensation with internal degrees of freedom in Alkali atom gases, J. Phys. Soc. Jpn. 67 (1998) 1822–1825.
[28] H. Pu, C.K. Law, S. Raghavan, J.H. Eberly, N.P. Bigelow, Spin-mixing dynamics of a spinor Bose–Einstein condensate, Phys. Rev. A 60 (1999) 1463–1470.
[29] D.M. Stamper-Kurn, W. Ketterle, Spinor condensates and light scattering from Bose–Einstein condensates, in: Proceedings of Les Houches 1999 Summer School (Session LXXII), 2001, pp. 139–217.
[30] J. Stenger, S. Inouye, D.M. Stamper-Kurn, H.-J. Miesner, A.P. Chikkatur, W. Ketterle, Spin domains in ground state spinor Bose–Einstein condensates, Nature 396 (1998) 345–348.
[31] T. Swislocki, M. Matuszewski, Controlled creation of spin domains in spin-1 Bose–Einstein condensates by phase separation, Phys. Rev. A 86 (2012), article 023601.
[32] M. Ueda, Y. Kawaguchi, Spinor Bose–Einstein condensates, arXiv:1001.2072v2.
[33] K.C. Wright, Stimulated Raman interactions in a spinor Bose–Einstein condensate, Ph.D. thesis, University of Rochester, 2009.
[34] S. Yi, Ö.E. Müstecaplioglu, C.P. Sun, L. You, Single-mode approximation in a spinor-1 atomic condensate, Phys. Rev. A 66 (2002), article 011601.
[35] R. Zeng, Y. Zhang, Efficiently computing vortex lattices in fast rotating Bose–Einstein condensates, Comput. Phys. Commun. 180 (2009) 854–860.